Nanoscale

Accepted Manuscript

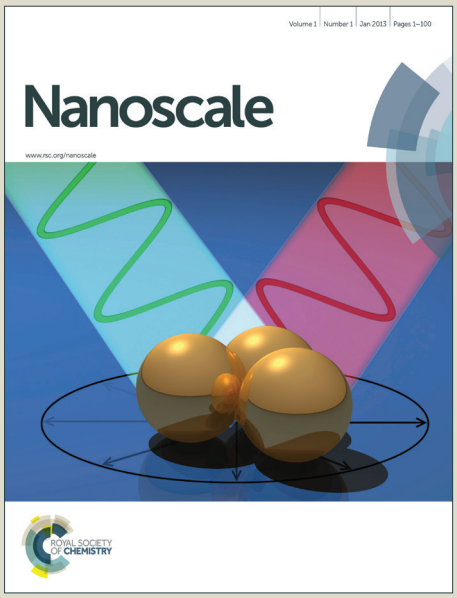

Surface Plasmon Resonance Mediated Photoluminescence Properties in Nanostructured Multicomponent Fluorophore Systems

Saji Thomas Kochuveedu and Dong Ha Kim[*]

Department of Chemistry and Nano Science, Global Top 5 Research Program, Division of Molecular and Life Sciences, College of Natural Sciences, Ewha Womans University, 52, Ewhayeodae-gil, Seodaemun-gu, Seoul, Korea.

[*]To whom correspondence should be addressed:

Tel: +82-2-3277-4124; Fax: +82-2-3277-3419; E-mail: dhkim@ewha.ac.kr

Abstract

The interaction between light and matter is the fundamental aspect of many optoelectronic applications. The efficiency of such devices is mainly dictated by the light emitting property of fluorophores. Unfortunately, the intensity of emission is adversely affected by surface defects, scattering and chemical instability. Therefore, enhancing the luminescence of fluorophores is necessary for better implement of nanocomposites in biological and optical applications. There are many interesting phenomena which can be observed if the characteristics of the fluorophores and metal nanoparticles are integrated. Photoluminescence (PL) by fluorophores can be enhanced or quenched by the presence of neighboring plasmonic metal nanostructures. An unambiguous study of the mechanism behind the enhancement and the quenching of emission is necessary to obtain new insight to the interaction between light and metal-fluorophore nanocomposites. In this review the core aspect of combining plasmonic metal nanostructures with fluorophores is discussed by considering various functional roles of plasmonic metals in modifying the PL property reported by various research groups. A few representative applications of SPR mediated luminescence are also discussed.

1. Introduction

Photoluminescence (PL) is the emission of light from a material upon photoexcitation. In a typical PL process a semiconductor is excited with energy larger than the bandgap energy. Once the photons of sufficient energy are absorbed, electrons and holes are formed at the conduction band (CB) and valence band (VB), respectively. Since the energy of excited electrons is high, they tend to return to the ground state and recombine with holes. During the recombination process of these photoexcited charge carriers, certain amount of energy is released in the form of heat or light energy. The light energy can be dissipated as radiation, which is observed as the luminescence and is characteristic for each material.[1 2, 3] In the case of dyes, the light emitting mechanism is the same, except that the CB and the VB are replaced by the highest occupied molecular orbital (HOMO) and the lowest unoccupied molecular orbital (LUMO), respectively.[3-6]

Semiconductor nanocrystals (NCs) attracted wide attention in recent years due to the ease to change their emission wavelength by tuning the size. The nanocrystal-based light emitters can be used for various applications such as opto-electronic devices[7-11] and biomedical diagnostics/therapy[12-16]. In order to make full advantage of the characteristics of nanocrystals, the control of PL property is very important. The emission properties of NCs are mainly dependent on the size of the crystal. Due to the quantum size effect, the bang gap of NCs increases with decreasing the size, leading to the shift of the band edge of PL from red to blue. Though fine tuning of the size may offer the control over the stability, emission color and brightness, most of the NCs suffer from less quantum yield (QY) due to surface defects and poor stability of NCs. Thus, it is necessary to find suitable strategies, which can ensure enhanced QY from semiconductor NCs in a stable and reproducible manner.

Recently, metal nanoparticles (NPs) have drawn particular interest since they can affect the fluorescence significantly when they are kept in close proximity of fluorophores.

Metal NPs have been reported to cause either radiative quenching or radiative enhancement depending on the size and the distance from the fluorophore.[6, 17-22] In general, quenching is observed when metal NPs are too close to the fluorophore,[21, 22] whereas separation by a certain distance leads to enhancement. This enhancement is based on the extent of interaction between plasmon resonance of metal NPs and fluorophores.[6, 17-19, 23] Such metal-induced improvement in emission is called metal enhanced fluorescence (MEF). MEF is primarily due to the near-field interactions of the excited emitter with the local electric filed around the metal NPs that is generated by incident light having appropriate wavelength.[6, 19, 23]

Noble metals such as gold (Au) and silver (Ag) are recognized for their unique surface plasmon resonance (SPR) property resulting from the interaction with light. Surface plasmons are the waves that propagate along the surface of the metal. When the wave vector of incident light is the same as that of oscillation of plasmons, these plasmons oscillate in resonance with the light. This resonant interaction between the SPs and the electromagnetic field of incident light leads to the phenomenon called SPR (Scheme 1).[24] The localized SPR (LSPR) band observed from nanostructured plasmonic metals can be tuned from visible to infra-red (IR) by adjusting the shape and size. This size and shape dependent spectral position of resonance gives vast opportunities to explore new aspects of underlying mechanism behind light-matter interaction, and to tailor them for specific applications.[25-28]

Modification of the PL of fluorophores by coupling with plasmonic metal nanostructures has drawn considerable attention because of the dramatic amplification in the emission of light from the emitters, which can improve their performance-based applications. The enhancement in the emission can be due to resonance energy transfer (RET)[29, 30] or near-field enhancement (NFE),[31, 32] and is primarily governed by the distance between the metal and the fluorophore. In the case of RET, the energy of the excited dipole can be transferred to the surface plasmons (SP). This transferred energy can then be absorbed by other dipoles,

leading to the formation of superradiant state (SR) that enhances the emission of photons.[30] Coupling of electromagnetic field of incident light with the oscillating electrons of plasmonic metal leads to strong enhancement of local electric field near the surface of the metal NPs. This enhanced field may interact with QDs or dyes, when they are kept closer to the metal surface, and may enhance the rate of exciton formation (Scheme 2).[33] These two mechanisms are discussed in detail in the later section.

MEF can be further used for the enhancement in the efficiency of Förster resonance energy transfer (FRET), since the presence of plasmonic metals can benefit the emission property of the fluorophore.[32, 34, 35] FRET is a photophysical process in which an electronically excited donor transfers its emission energy to a neighboring acceptor by nonradiative dipole-dipole interaction.[4, 5] A typical FRET system constitutes a donor-acceptor pair, where the emission wavelength of the donor should be overlapped with the absorbance wavelength of the acceptor.[4, 36] High molar absorptivity and high QY are the other essential requirements for efficient FRET.[34] However, most of the FRET systems suffer from poor QY and low photostabiltiy, which in turn affect FRET efficiency adversely.[34] Placing plasmonic metals in the close vicinity of donor or acceptor may open facile routes to improve the effectiveness of emission of the donor or the acceptor through the aforesaid mechanisms, ultimately leading to an enhancement in FRET efficiency.[6, 37]

In this review we try to study the recent development of various nanohybrid systems consisting of light emitting materials combined with plasmonic nanostructures and the mechanism behind the energy transfer from plasmonic nanostructure to light emitting materials such as QDs and dyes or vice versa. Here, we focus on the underlying science in MEF rather than the technical aspects of fabricating nanohybrid structures and their specific applications. The mechanism behind energy transfer is organized as different sections and discussed them in detail. A few selected applications based on SPR-induced enhanced

emission are also discussed at the end of the review.

2. Photoluminescence (PL)

PL is the emission of light from any substance, and occurs from photoexcited states. When light of sufficient energy is incident on photoactive material, photons are absorbed and excited states are created.[1, 2] Direct bandgap semiconductors possess a void energy region where no energy levels are available for the electron to exist. This void region, between the top of the filled valence band (VB) and the bottom of the vacant conduction band (CB), is called the band gap. The light absorption characteristics and photocatalytic efficiency of the semiconductors are decided by this band gap. Semiconductors are transparent to photons whose energies lie below their band gap and are strongly absorbing for photons whose energies exceed the band gap energy. Band-to-band absorption involves excitation of an electron from the VB to the CB resulting in the creation of electron-hole pairs. The electron-hole pairs created when the photon was absorbed by a semiconductor undergoes the recombination, resulting in the emission of light (Scheme 3).[38, 39]

PL involves more processes when the light emitting material undergoes internal energy transitions before re-emitting the energy. Luminescence is broadly divided into two - fluorescence and phosphorescence, based on their energy transitions. The excitation of fluorophores and subsequent emission can be well described using the Jablonski diagram (Scheme 4). Fluorophores are excited from ground state (S_0) to higher vibrational level (S_1 and S_2) after absorption of light. The fluorophores then relax to lower vibrational level through a process called internal conversion. Fluorophores may come back to the ground state by the emission light called fluorescence, or undergoes a spin conversion called intersystem crossing, which causes a spin conversion from singlet (S_1) to triplet (T_1) state. The molecules then come to ground state by the process called phosphorescence.[3, 4]

The energy of the excited electrons can be decayed mainly through two pathways,

i.e., radiative decay and non-radiative decay. Spontaneous emission of photons in all directions is called radiative decay, which reduces the lifetime of the emitter. Fluorophores however are sensitive to their distance with quenching agents and other environmental changes (pH, temperature, polarity, oxidation state and other factors). Energy loss due to these factors is known non-radiative decay.[4, 6] Non-radiative and radiatve decay combinely decide the quantum efficiency. The presence of metals in the close proximity of the emitter can alter the rate of this radiative and non-radiative decay rate, and thereby the intensity of emission.

2.1 Radiative decay

The spontaneous emission of light from the luminescent materials is a process of returning to the ground state through radiative decay. During the transition of electrons from higher energy state to an empty lower energy state, most of the energy difference between the two states can be decayed as electromagnetic radiation. The luminescence quantum yield is defined as the ratio of number of photons emitted to the number of photons absorbed. The presence of metals in the close proximity of the fluorophore or semiconductor can alter the radiative decay rate of the emitter, and thereby the quantum yield. This is due to the interaction of the excited state of the emitter with the free conduction electrons of the metal.[40] When the radiative decay rate increases, quantum yield increases and life time decreases. Metal-induced increase in radiative rate can enhance the emission of luminescent materials. The radiative decay rate of the emitter is normally the fundamental property of the emitter. The metal induces a dipole in another particle in response to its own dipole. The coherent sum of these dipoles is responsible for the net emission of the acceptor and is due to the direct coupling between the dipole field and surface plasmon polaritons (SPPs).[41] SPPs are the wave modes which travel along the metal-dielectric interface. The field generated by SPPs decay exponentially as the distance increases from the interface (Scheme 5).[42, 43] The coupling

increases the momentum of the mode, which is greater than that of free photons, and is maximal for a small but finite separation between the emitter and the metal surface. When the emitter is away from the metal, then coupling to non-radiative mode is negligible, and the radiative decay overrules. The size of the metal NPs also play a pivotal role in radiative decay. The extinction of metal nanostructures is composed of absorption and scattering and the degree of contribution of these two components depends on the nature and size of the metal. The extinction of metal NPs having size below 20 nm is mostly due to absorption and such particles tend to quench the fluorescence, whereas scattering efficiency is high in the case of bigger NPs, thus enhancing the radaitive decay.[44]

2.2 Non-radiative decay

It is possible for the excited electrons of the emitter to return to the ground state in a non-radiative manner. The non-radiative energy can be lost to the local vibrations of surrounding atoms and the excess energy may dissipate as heat.[1] When the emitter is very close to the metal surface, non-radiative decay process induces the energy transfer from the excited dipole of the emitter to the metal, resulting in the quenching of emission. If the transfer takes place to the dipole of the metal, the plasmons of the metal can be excited. Again, the nature of the metallic surface can alter the radiative and non-radiative decay. Metallic nanoparticles with small radii of curvature increase the coupling between dipole of the emitter and SPPs of metal, resulting in an increase in non-radiative decay followed by quenching of emission. Strouse and coworkers studied quenching of fluorescence using smaller metal NPs. They reported that when the size of the NPs is below 2 nm, quenching is observed due to the coupling of the oscillating electronic dipole of a dye to a metal surface, resulting in non-radiative loss of energy. Due to the small radii of curvature of very smaller NPs any free electron traveling within the NP has the highest probability of scattering normal to the surface compared to any other orientation. As in the case of FRET this perpendicular orientation of

dipoles leads to quenching of emission.[45, 46] In the case of bigger metal particles, the possibility of scattering from the metallic surface leads to the coupling of SPPs to radiation, which increases the radiative decay.[42] Pockrand *et al.* studied the distance dependence of the coupling between the emitter and SPPs and they considered the maximum coupling distance as 20 nm,[47] which was further reported by Lakowicz.[44] Another non-radiative decay channel is explained by the induced charge separation at the metal-emitter interface. When the emitter is close to the metal, the charges are closely packed, and then the plasmon cannot be radiated. Instead, they decay into heat, resulting in the quenching of the emission.[44]

3. SPR-mediated enhancement of PL

The ability to trap and concentrate light makes plasmonic metal NPs a potential candidate in MEF. Typically, either Au or Ag nanostructures are used since their SPR wavelength can be tuned from visible to infrared by merely changing the size and shape. Chemical or physical stability of these metals also makes them a recommendable choice in fabricating MEF system. Due to the coupling between the oscillating electrons of the light emitter and the surface plasmon of metal NPs, a strong enhancement in fluorescent emission is obtained.[48] An overlap of the absorption wavelength of the metal and the emission wavelength of the emitter is a preferable requirement for the efficient MEF since it allows a viable excitation and energy transfer.[49-51] The degree of enhancement is dependent not only on the spectral overlap but also on the position and orientation of the emitters with respect to the metal NPs.[32, 52] Plasmonic fluorescence enhancement has been reported by many groups using different types of plasmonic nanostructures. By controlling the size or shape of the metal nanostructures, the interparticle distance, concentration and spectral relationship between the emitter and the metal NPs, MEF can be improved due to the efficient energy transfer from the metal to the fluorophore and increased rate of exciton formation induced by NFE.

Interaction between the plasmonic and excitonic system is explained using classical

electromagnetic method as follows. When quantum emitter is in the close proximity of plasmonic nanostructures, hybridized states are formed due to the interaction between the two objects. The resultant wave functions are the mixture of the collective plasmon mode and the exciton, which is sometimes called as plexcitons.[53, 54]

3.1 Resonance energy transfer

When an excited emitter is located in close proximity to a metal, the energy of the emitter can be transferred to the metal followed by dissipation and radiation. In the case of RET, the emission of fluorescent molecules, *e.g.*, QDs or dyes, first radiatively excites surface plasmons (SPs) in the metal, which then non-radiatively transfers the energy to the emitters, leading to a cross talk between the emitters. The major cause of RET is the electromagnetic interaction between the dipole of the emitter and plasmons of the metal nanostructure. This mechanism explains the emission of light by an ensemble of dipoles of emitters located near the metallic NPs. Emission of photons is the result of RET between these individual dipoles and SPs. Therefore, emission of photons is a cooperative process involving all the dipoles in the ensemble and the NP (Scheme 6).[30] This SP-induced coupling between the dipoles leads to the formation of SR states that enhances the emission of fluorophores. Since SPs extend throughout the metal-fluorophore system, the metal nanostructure may act as pool that couples near and far dipoles uniformly throughout the ensemble. Due to this effective hybridization, the emission of photon becomes a cooperative process between all the dipoles in the fluorophore and metal NPs.[30, 55] RET can be controlled by tuning the size and shape of the plasmonic NP, since they influence the electronic distribution around the NPs. The interaction and efficiency of energy transfer may vary depending on the distance vector between the emitter and the metal. At a shorter distance, radiative energy of emitter is absorbed by the metal NPs to excite the plasmons, resulting in quenching of the fluorophore emission, whereas at an intermediate distance the aforementioned cooperative process

between the metal and the emitter dominate, giving rise to an enhancement in the emission of the fluorophore. It is reported that this energy transfer process follows a variable distance dependence of $1/d^4$, where d is the distance between the metal and the emitter.[29, 30, 55-65]

3.2 Near-field enhancement (NFE) mechanism

Radiative energy transfer from the metal to the fluorophore can take place through enhanced electromagnetic near-field via SP excitation. Strong electric fields are generated around the excited plasmonic NPs and the magnitude of the field is significantly enhanced than that of photons used to photoexcite the nanostructure. The field associated with SP is sensitive to the variation in the dielectric environment around the NPs.[66] Plasmonic metallic nanostructures can act as antennas by concentrating the electromagnetic field around the sharp corners of the nanostructures.[67] The physical origin of NFE can be due to the collective oscillation of plasmons.[68] The strength of the field is highest near the surface of the plasmonic nanostructure and decreases exponentially away from the surface. The field enhancement factor is reported as 10 up to 10^6 times larger than the incident field, depending on the morphology and the surrounding medium of the metal system.[69, 70] The highest NFE is found for geometrical systems, where metal NPs are uniformly distributed and at an interacting distance from each other. When the surface plasmon absorbance wavelength of metal nanostructure is close to the excitation wavelength of light emitter, the excitation of the emitter can be enhanced due to NFE arising from the SPR.[31] The NFE around the excited plasmonic nanostructure can excite the fluorophores, ultimately resulting in the enhancement of the emission of fluorophores. The excitation enhancement factor is proportional to the local field intensity.[31, 71] The enhancement in fluorescence intensity is dependent on the distance and orientation of the fluorophore relative to the metal nanostructure.[70] This dramatic increase in fluorescence emission can amplify the emission signal of weak fluorophores.[66] When an excited dye is placed very close to the metal, its fluorescence rate

and fluorescence life time are changed because of the radiative loss of the dye to the non-radiating plasmons of the metal NPs,[70] and in addition, both radiative and non-radiative rates are affected owing to the changes in the optical local density of states created by metal NPs.[32] It is reported that the emission enhancement is due to the increase in radiative decay rate.[31, 32, 72]

In the case of dyes the absorption and emission wavelengths are close to each other, and when the plasmon resonance peak of noble metals are comparable to the emission peak width of the dyes, the excitation and emission enhancements can occur simultaneously. The total enhancement factor depends on the relative overlap of the plasmon wavelength to the excitation and emission wavelengths. When QD/dye is in close proximity of metal NPs, quenching of emission may also occur. Fluorescence quenching is significantly larger in the case of smaller metal NPs since the magnitude of near field enhancement is not enough to enhance emission. When the magnitude of local field enhancement is large, it outdoes the quenching effect, eventually leading to an enhancement in the emission.[31] Hsieh *et al* studied emission enhancement and quenching of CdSe in the presence of Au NPs. Initially emission of CdSe is enhanced as the concentration of Au NPs is increased owing to the increased near field by plasmons. However, quenching of emission is observed when the concentration of Au NPs exceeds a certain threshold, which is attributed to the decrease in distance between the CdSe and Au NPs, leading to the electron transfer from QD to metal since the excited electrons and holes can tunnel to the plasmonic NPs through non-radiative relaxation.[71] Song *et al* argued that metal nanostructures whose extinction is dominated by plasmonic absorption usually lead to quenching, whereas when their extinction is dominated by scattering they may enhance the quantum yield. They prepared lithographically patterned plasmonic arrays of 100 nm sized Ag arrays, which can support both localized and propagating SPP modes, and they observed that the SPPs are highly radiative when the individual Ag particles are strongly

interacting with each other. When light is incident on such interacting spots, enhanced local fields are induced, which in turn enhances the formation of electron-hole pairs. While the Ag NPs are non-interacting, the dipole-dipole interaction between the NPs is weak and the radiative scattering efficiency is not enough to overcome the plasmonic absorption components, resulting in rather minimal enhancement. The SPPs become active when the NPs are at an interacting distance, and the incident light is absorbed and scattered efficiently, leading to an enhanced local field around the coupled region. Generation of electron-hole pair is significantly increased when the enhanced scattering field is absorbed by QDs.[73] This scattering induced enhanced field was further explained by Giannini *et al*. They reported that when the scattering cross section is bigger than the geometrical cross section, the energy of the incident field around the metal nanostructure is concentrated, leading to a local enhancement of the electromagnetic field.[74]

Another cause of enhanced emission of fluorophores is the existence of 'hot spots' between the plasmonic metal NPs. Since nanostructures can act primarily as nano antennas to concentrate the light energy surrounding them, the intensity of the coupled electric field is several folds larger when two plasmonic nanoparticles are interacting with each other, compared with the magnitude of electric field where the plasmonic NPs are non-interacting. Such local areas, where intensified electric fields exist, are known as hot spots. Though the simplest system on which hot spots can be studied is a dimer,[75] the junction between adjacent nanoparticles, available in pairs, clusters or even aggregates can also generate intensified localized field when they are excited by light of appropriate wavelength and polarization (Figure 1).[54, 76] Recently a few works addressed the enhancement of fluorescence when fluorophores are placed between two plasmonic nano-objects. Bek *et al* compared the enhancement in fluorescence in the presence of single Au NP with that in the presence of dimer, where they observed the increase in the fluorescence intensity by 270 %, which is

more than the sum of the effect of two non-interacting Au NPs. When the fluorescent sphere is not located on the connecting axis of the two Au NPs, the degree of enhancement is weakened, confirming the presence of hot spots between the NPs (Figure 2). The effect of hot spots is experienced even when the two Au NPs are separated by ~ 40 nm.[75] Muskens *et al* reported a new class of NP design called optical antennas, which can combine radiative efficiency with geometric resonances and NFE in the gap between the optical antennas. It was found that the enhancement of both decay rates and quantum efficiency is weaker than that for the coupled antennas. They investigated further by coupling more antennas in the cluster, which further improved the quantum efficiency.[52] Zhang *et al.* synthesized Ag NPs, which were then chemically attached to oligonucleotide 1. The labeled metal monomers were achieved by the hybridizations between the bound oligonucleotide 1 and labeled oligonucleotide 2, and the metal dimers were obtained by hybridization between the metal bound oligonucleotide 1 and labeled double-length oligonucleotide 3 (Scheme 7). They obtained 7-fold and 13 fold fluorescence enhancement on the metal monomer and dimers, respectively. This result is attributed to the enhancement in the electric field intensity between the metal dimers, induced by the coupling effect of dimers.[23] A maximum enhancement of fluorescence quantum yield can be obtained only when the fluorophore is at an optimum distance from the metal surface.[77] Metallic nanostructures with sharp edges are also able to produce concentrated enhanced field at the edges. 'Bowtie' nanoantennas consisting two tip-to-tip, separated by a small distance, can produce large electric field confined to the area near the gap.[78, 79] Kinkhabwala *et al.* reported large enhancement in single molecule fluorescence in bowtie nanoantenna, and observed up to 1,340 times enhancement in the emission of dye, which was incorporated onto the surface of bowtie nanoantennas.[79]

4. SPR-mediated quenching of PL

Although the MEF can be expected when plasmonic metals are kept in the proximity of fluorophores, quenching is also observed when the metal is located close to the fluorophore and the size of the NPs is too small. The change in emission property is influenced by the radiative decay rate due to photon emission and by the non-radiative decay rate due to energy dissipation such as heat or collision of photons with metal surface etc.[80] Quenching is most often observed when the metal-fluorophore distance is less than 6 nm, whereas enhancement is reported when it is between 6 to 10 nm.[81] When the fluorescent molecules are located at very close distance from the metal surface, non-radiative energy transfer from the flourophore to the metal takes place, which in turn decreases the quantum yield, resulting in the quenching of emission.[22, 59, 82] The radiative decay rate is reduced during quenching of the emission, owing to the out-of-phase orientation of molecular dipoles of the fluorophore and the dipoles induced on the plasmonic metal.[22] Reineck *et al.* studied the fluorescence quenching of four different dye molecules, which absorb light at different wavelengths ranging from the visible spectrum to the near infrared, using a rigid silica shell as a spacer. The quenching is caused by energy transfer from the fluorophore to higher-order localized surface plasmon modes in the Au NPs. The most efficient energy transfer occurs for an emitter whose emission wavelength is very close to the surface plasmon band of Au NPs. One of the well-studied mechanisms, which govern the non-radiative energy transfer to metal NPs, is the nanometal surface energy transfer mechanism.[21]

4.1 Nanometal surface energy transfer (NSET) mechanism

As discussed earlier, when the fluorophore is kept in very close proximity of the plasmonic metal, the emission energy of fluorophores can be transferred to the metal, leading to quenching. Unlike the case of RET, NSET does not require any resonant electronic transition.[46, 83] NSET is originated by the interaction of electromagnetic field of the fluorophore dipole interacting with the free conduction electrons of the metal, is more often

observed in the case of smaller NP and is relatively short-range effect.[84] In metallic nanostructures these conduction electrons may behave as an acceptor. Electrons travelling within the NP may scatter normal to the surface as opposed to any other orientation due to the higher curvature of smaller NPs and interact strongly with the dipole of the fluorophore when they are perpendicular (Figure 3a-b). This interaction increases the total non-radiative rate of the dye, and reduces the lifetime and quantum yield of the fluorophore.[45, 83] Karthikeyan also studied the same mechanism using rhodamine-6G doped Au-polyvinyl alcohol nanocomposite polymer films. In addition to the NSET mechanism, he proposed electron transfer mechanism, where nonradiative energy transfer of electrons at energies close to the Fermi level of Au occurred (Figure 3c). This process increases the nonradiative rate of the dye and reduces the quantum yield, leading to the quenching of emission.[83]

5. SPR-induced enhanced FRET

5.1 FRET

FRET is an energy transfer from an excited donor to a ground state acceptor in a non-radiative manner through dipole-dipole interaction (Scheme 8). In FRET, a donor absorbs energy and is excited followed by the transfer of the emission energy to the nearby emitter, the acceptor. This energy transfer manifests a decrease in the emission intensity of the donor, associated with a reduction of the excited lifetime, and an enhancement in the emission intensity of the acceptor.[4] The rate of energy transfer depends on the spectral overlap between the emission energy of the donor and the absorption energy of the acceptor.[36] The distance between the donor and the acceptor, and the relative orientation of the dipoles of donor-acceptor pair, are the other important dependent factor for effective FRET (Scheme 9).[34, 85] An excited fluorophore is considered as an oscillating dipole, which can exchange energy with other dipoles of similar frequency. A pair of emitters involving in this non-radiative energy transfer is known as donor-acceptor pair.[86]

In recent years, considerable research efforts have been devoted to FRET, which is extensively used in the study of various biological phenomena, such as protein-protein interactions,[4, 87, 88] and conformational changes of biomolecules.[89, 90] Since FRET can give valuable information on the spatial orientation relationship between fluorophore-labeled biomolecules, FRET imaging has become a successive analytical tool to investigate the molecular interactions in living organisms. However, FRET is a very short range effect (<10 nm), and only observed when the donors and acceptors are in very close proximity. The FRET efficiency is drastically decreased when the Förster radius is beyond 5 nm, which limits its use in biological or biomedical applications since the range of biomolecular interaction is longer than this range.[34, 62]

MEF and consequently influenced FRET is an advanced technique to enhance the florescence intensity of the acceptor and to increase the Förster range. Enhanced fluorescence due to the presence of plasmonic metals helps to detect lower concentration of biosystems marked with fluorophores.[91] When the donor or acceptor of a FRET system is placed close to the metal, the fluorescence of corresponding component is enhanced due to the electromagnetic coupling of the fluorophore with the nearby metal nanoparticle.[56, 92] However, if the distance between the metal and the fluorophore is too small (<5 nm), quenching of the emission is observed due to the energy transfer from the fluorophore to the metal. Therefore, careful tuning of the distance between the metal and the fluorophore is a prime requirement for the effective MEF.[80, 93]

5.2 FRET influenced by SPR

The interaction of an emitter with plasmonic nanostructures has drawn remarkable attention because plasmons oscillating in the visible region can influence the oscillating dipoles of the acceptor or donor of the FRET system.[32] Metal NPs can alter the radiative and non-radiative decay rate of the emitter because of the change in the optical field induced by the plasmonic

metal. Excitation of SPPs within metal NPs can create strong optical fields. The changes in the FRET system induced by SPR depend on the size and shape of the plasmonic nanostructures, the interparticle distance, and the relative spectral characteristics between the donor and the acceptor with plasmon absorption features of the metal. If the donor or acceptor of a FRET pair is in direct or close contact with the metal surface, quenching of the emitter is observed due to the non-radiative energy transfer to the metal. It can be generally summarized that quenching is observed when extinction coefficient is dominated by plasmonic absorption, whereas enhancement in emission is obtained when extinction is dominated by scattering.[73] Therefore smaller metal nanostructures usually tend to cause quenching of emission compared to bigger nanostructures. Locating the metal NPs at an appropriate distance from the acceptor or emitter can enhance the FRET. When the metal NPs are close to the donor, the emission of donor is enhanced, and then the enhanced energy can be transferred to the acceptor. Placing the metal near the acceptor enhances the emission of the acceptor through two ways. One is through MEF and the other is through energy transfer from the donor to the acceptor via FRET. The overall enhancement in FRET induced by SPR can ultimately increase the Förster radius (R_0), which is the distance at which 50 % energy is transferred from the donor to the acceptor.[34, 35]

5.2.1 SPR-induced enhancement in FRET

It has been reported that LSPR of metallic nanostructures can enhances FRET property via dipole-dipole interaction mechanism.[94] Here, the emission property of the acceptor or donor is altered via localized fields created by plasmonic nanostructures and increases the strength of the donor-acceptor interaction.[34, 95, 96] Increase in R_0 with the aid of plasmon coupling is reported by a few groups.[34, 35] When a plasmonic nanostructure is present in the vicinity of the fluorophore, the intensity of the emission of fluorophores can be varied in two ways. One is the increase in excitation rate by the local electric field induced by LSPR, and the other is

the increase in decaying the energy through non-radiative pathway.[97] As the excitation and emission of the fluorophore can be altered by SPR, the excitation and de-excitation processes of a FRET pair are also modified subsequently. The plasmonic nanostructures can change the emission decay rate of the donor and the acceptor which includes energy transfer from the donor to the acceptor and that between the metal nanostructure and the fluorophore. In addition, it has been reported when there is an overlap between the plasmon resonance peak and the emission spectrum of the fluorophore, increased fluorescence intensity is observed due to the plasmon-induced enhancement in emission.[31, 79, 97]

Zhao *et al* studied the influence of SPR on the energy transfer rate (k_{ET}) of the donor and the sum of radiative and non-radiative decay (k_D).[97] The enhancement of k_{ET} depends on the size, shape, plasmon wavelength and position of the donor-acceptor pair relative to the plasmonic nanostructure.[41, 96-98] They reported the influence of SPR on FRET using Au-Ag core-shell nanostructures coated with silica shell, onto which the donor and acceptor moieties are embedded. The enhancement in k_{ET} and k_D was changed by changing the plasmon wavelength of the metal nanostructures. They argued that when the plasmon peak overlaps with the emission peak of the donor, k_D is enhanced, while k_{ET} is not considerably enhanced, leading to a decrease in the energy transfer efficiency (E). The enhancement in k_D may cause quenching of fluorescence. When the plasmon peak was placed between the emission peak of the donor and the absorption peak of the acceptor, k_{ET} is considerably enhanced, which increases overall E. Lunz *et al.* compared FRET with and without Au NPs using multilayer sandwich structure, where QDs are used as both donor and acceptor. The Förster radius was increased from 3.9 to 7.9 nm and the FRET rate was increased by 80 folds for the structure with Au compared to that for the structure without Au. They argued that donors with the wavelength of emission spectra in resonance with the SP absorption wavelength of Au NP monolayers showed SP-mediated energy transfer, which led to the enhancement of emission

of the acceptor.[99] This is contradictory to the finding of Zhao *et al*.[97] Faessler *et al.* used 40 nm Au NPs as plasmonic nanoresonators, and FRET conjugates were attached to monomer and dimer Au NPs to study the influence of hot spots on FRET. FRET conjugates at the hot spot of a dimer experienced better FRET enhancement compared to a FRET conjugate attached to the monomer.[100] Using 15 nm Au NPs, plasmon-mediated non-raditive energy transfer between QDs via FRET was studied by Ozel *et al*. Selective plasmon-mediated energy transfer via FRET was studied using controlled plasmon coupling either only to the donor or only to the acceptor. It was observed that the acceptor selective plasmon coupling led to higher acceptor emission enhancement compared to the donor selective plasmon coupling.[100] Reil *et al.* studied enhancement in the acceptor luminescence at the expense of the donor emission by locating metal NPs on the donor-acceptor pair. The electromagnetic field near the metal NP leads to enhancement of the radiative decay rate. The degree of enhancement of the donor emission is less compared to that of the acceptor emission (Figure 4). The reason why the enhancement of the donor emission is not that significant is the decrease in the QY associated with ohmic losses in the MNP, whereas the QY of the acceptor is enhanced in the presence of the MNP, resulting in an enhancement of the acceptor fluorescence. It was further explained that by tuning the plasmonic resonance wavelength of the metal NP close to the emission wavelength of donor, part of the near field energy of the donor can be converted into light by the metal NP, at the expense of the Förster energy transfer and other non-radiative processes.[32] Su *et al.* analyzed plasmon-assisted energy transfer between QDs using SiO_2 coating as the spacer between Ag NP of size 170 nm and QDs, and obtained 86 % FRET efficiency when the thickness of SiO_2 is 7 nm. This enhancement was attributed to the faster radiative decay and the enhanced radiative emission due to the effect of plasmon-induced field enhancement.[101] The same group reported 88 % of FRET efficiency using Ag NPs of 110 nm size with silica thickness of 7 nm.[102]

5.2.2 SPR-induced quenching in FRET

Even though most of the SPR based FRET studies are focused on the enhancement of the acceptor emission in FRET, there are a few reports on the quenching of FRET in the presence of metal NPs. Kim *et al.* studied switching-off FRET by plasmonic effects. Donors and acceptors of a FRET pair were incorporated into the different blocks of an amphiphilic diblock copolymer. To study the effect of surface plasmons, a layer of silver NPs was spin coated on a suitable substrate, onto which polymer solution containing donors and acceptors was spin coated. It was observed that the fluorescence spectra of the donor and the acceptor remained unaltered compared to the fluorescence spectra of the polymer containing either only the donor or acceptor. Excitation of surface plasmons of Ag NPs creates a strong electromagnetic field, which can increase the excitation rate of the donor and the acceptor in the vicinity of Ag. Meantime, the excited-state energy of fluorophores can be transferred to metal NPs and then dissipated as heat by NSET mechanism (Figure 5). The FRET was retrieved by introducing a spacer layer between the metal and the polymer film incorporated with donor-acceptor pairs. They concluded that switching-off FRET is mainly caused by the NSET decay process by the proximity of fluorophores and metal NPs.[103] Zhang *et al.* also studied the effect of NSET in a metal-fluorophore system. Five differently sized QDs were prepared to study the quenching effect by surface plasmons. The quenching of emission of QDs was maximal when the thickness of the spacer between Au NPs and QDs is minimized, and when the concentration of Au NPs was higher. It was suggested that the quenching is due to the non-radiative energy transfer to metal NPs.[104]

5.2.3 Effect of the position of plasmonic nanostructures in FRET system

Although various groups mainly studied that combining SPR with FRET pairs increases the FRET rate between donor-acceptor pairs through plasmon coupling, the influence of spatial location of plasmonic nanostructures on the emission property is investigated by only a few

groups.[94-96, 99] Enhancement of FRET by placing metal nanostructures between the donor and the acceptor was demonstrated by a few groups.[94-96, 99] Lunz *et al.* prepared multilayer structures consisting of monolayers of donors, acceptors and Au NPs, separated by polyelectrolytes. In the presence of Au NPs, the donor emission was reduced by 13 %, while the emission of the acceptor was increased by 24 %, with the donor-acceptor center-to-center separation of 23 nm. No FRET was observed with a similar structure without Au NPs, since the distance between the donor and the acceptor was too large for the energy transfer to take place.[99] The same group studied the effect of Au concentration in the multilayer sandwich structure, where it was observed that the emission of the acceptor was enhanced when the concentration of Au was at a low to intermediate level, and decreased at higher concentration of Au due to dominant direct quenching by the Au NPs.[94] Ozel *et al.* explored the effect of SPR on FRET using donor- or acceptor-selective coupling of SPR. They controlled plasmon coupling either to the donor or to the acceptor, and studied plasmon-mediated energy transfer from the donor QDs to the acceptor QDs. They controlled the plasmon interaction structurally through placing the plasmonic layer either close to the donor or to the acceptor to probe the donor-plasmon coupling or the acceptor-plasmon coupling, respectively. The donor-selective plasmon coupling enhanced the acceptor emission by a factor of 1.93, whereas the acceptor-selective plasmon coupling led to 2.70 fold enhancement in the acceptor emission, which is due to the acceptor plasmon coupling and FRET-assisted energy transfer from the donor to the acceptor (Figure 6).[95]

Viger *et al.* opted to position the acceptor closer to the metal coated with silica shell, because the quantum yield of the acceptor (eosin) is reported to be less compared to that of the donor (fluorescein isothiocyanate).[34, 35] In the presence of the metal, the Förster radius was increased from 5.5 nm to 7.5 nm, and the Förster efficiency was increased by a factor of 4.[34] They extended their work by changing the fluorescein isothiocyanate as acceptor and

employing a new donor, a cationic conjugate polymer. Again, the acceptor was placed near the plasmonic metal. It was observed that the Förster radius was increased from 5 nm to 8.5 nm and the Förster efficiency by a factor of 13, respectively, when the plasmonic metal was included.[35]

6. Plasmon controlled fluorescence: Applications

The interaction of fluorophores with plasmonic nanoparticles has attracted significant attention correlated with numerous applications, especially in life science. MEF in fluorescence and FRET is a practical tool utilized in various applications such as optical display,[61, 63, 105] biosensing,[19, 106, 107] photodynamic therapy[108-110] etc. This enhancement along with reduced lifetime and improved quantum yield lend them feasibility for the above-mentioned applications. Protein sensing is one of the widely studied applications of MEF and FRET. As plasmonic metals have sufficient binding affinity to proteins, enhanced fluorescence by metal NPs can improve the detection signal.[19] Another upcoming area where MEF can be widely exploited is the photodynamic therapy. Photodynamic therapy involves the combination of fluorophores known as photosensitizers (PS). By absorbing light PS produces reactive oxygen species that can damage cellular constituents. The presence of metal nanostructures can amplify the production oxygen radicals and the detection signal.[108] The third commonly explored use of MEF is in display devises, especially organic light emitting diodes (OLEDs). The surface plasmons are used to mediate energy transfer from the plasmonic metal to fluorescent dye molecules.[57] In this section the SPR-mediated applications are classified into two categories, biomedical and display applications. Biomedical application is subdivided into biosensing and photodynamic therapy. In display section the discussion is focused on SPR-mediated enhanced emission from LEDs and OLEDs

6.1 Biomedical applications

6.1.1 SPR-enhanced fluorescence for biosensing

SPR-induced enhanced fluorescence is considered as an apt analytical tool for protein sensing. In conventional protein sensing, fluorophores, which are covalently labeled to proteins, are the suitable probes. Most of the cases, these fluorophores undergo quenching due to energy transfer between nearby fluorophore molecules.[111] The Förster distance for homo FRET is below 5 nm, which is larger than the length of many proteins. Energy transfer between the fluorophores is expected to take place when the assay contains more than one fluorophore. This adversely affects the detection of labeled antibodies used in immunoassays since self-quenching of emitters reduces the brightness of the labeled target molecules. It has been reported that the self-quenching can be reduced to a significant extent in the presence of plasmonic metal NPs, which is attributed to the increase in radiative decay.[91]

Lakowicz and co-workers performed extensive research in MEF-induced enhanced biosensing.[91, 112-114] Self-quenching was reduced when fluorescein-labeled human serum albumin (HSA) was bound to a Ag island film. This is due to the interaction of the fluorophore with free electrons of the metal, which increases the quantum yield and the radiative decay.[91] Similar enhancement in the emission of fluorescence was observed when indocyanine green (ICG)-labeled HSA was bound to a Ag film.[112] An increase in the fluorescence intensity by 18 ~ 80 times with one-photon excitation and up to several hundred fold or larger with two-photon excitation was obtained when labeled avidin molecules were adsorbed on a Ag film surface (Figure 7).[114] MEF was further used to study DNA hybridization by binding thiolated oligonucleotides to Ag particles on a glass substrate. 12-fold increase in fluorescence intensity was obtained during hybridization when complementary fluorescein-labeled oligonucleotides were added.[113]

Sokov *et al.* studied the enhancement of emission of biotin-fluorescein conjugates captured on alternative layers of bovin serum albumin-biotin (BSA-biotin) conjugates and

avidin. An enhancement factor of 20 was obtained when the protein layers were deposited on a Ag film.[77] Xie *et al.* investigated the fluorescence enhancement using a monolayer of FITC-conjugated HSA (FITC-HSA) attached to Ag, which was deposited on Au colloid surface immobilized on a glass surface by covalent bonding. Fluorescence of the fluorophore (FITC) was quenched, unaffected, or enhanced in comparison to the control, depending on the size of Ag NPs. The size dependent enhancement of fluorescence was attributed to the effect of increased excitation rate from the enhanced electromagnetic field around the Ag NPs and a higher quantum yield from an increase in the intrinsic decay rate of the fluorophore. Amplification of the fluorescence intensity using Ag nanowires was explored by binding FITC-HSA to the glass surface covered with Ag nanowires, which is several micrometers in length and 50-100 nm in diameter.[115] They argued that the fluorescence enhancement is not only due to the greatly increased total surface area and aspect ratio of Ag nanowires, but also the enhancement of the electric dipole moment for electron resonance oscillations along such wires. Coupling of the optical dipoles in the fluorophore molecules to these resonance oscillation may result in nanoantenna effects where the coupled radiation is effectively re-emitted to the free space.[107, 115] The effect of the distance between the metal particles and the size of the NPs on the fluorescence enhancement was studied by binding monolayers of FITC-HSA and deep purple-conjugated BSA (DP-BSA) to Au NP surfaces, which have either larger or smaller interparticle distance. It was observed that the fluorescence enhancement in the samples with closely arranged Au NP monolayers is generally much higher than that from the well-isolated NPs (Figure 8). This is attributed to the effective localization of the electromagnetic field in interparticle regions, which leads to the effective coupling of the localized field, and further leads to the enhanced fluorescence.[116]

6.1.2 SPR-enhanced fluorescence for photodynamic therapy

Photodynamic therapy (PDT) is a recently developed therapeutic option for the treatment of

cancer. PDT consists primarily of three components: photosensitized drug, light and oxygen. After absorbing light the photosensitizers (PSs) transfer the energy to oxygen molecules to produce singlet oxygen or to surroundings to produce free radicals. The singlet oxygen species are cytotoxic in nature, which can damage cellular components, ultimately leading to the death of cancer-affected cells (Figure 9).[108, 109] The overall process involved in PDT is as follows: first the dye in the ground state (S_0) is excited to an excited singlet state (S_0), which is then transferred to a triplet state of the dye by intersystem crossing. The collisional energy transfer from the triplet state of the dye to the ground-state molecular oxygen produces reactive singlet oxygen. Owing to this, tumor cells can be selectively located and destroyed (Figure 10), thereby severe side effects of chemotherapy can be avoided.[110, 117, 118] PDT is effective within the availability of singlet oxygen. All the tumor cells are not killed if the singlet oxygen supply is insufficient, whereas excess supply may kill or damage healthy cells around cancer-affected cells. In this regard, MEF can be used as efficient means to control the amount of singlet oxygen generation through metal-PS interactions. Enhanced electromagnetic field around the metal is the basis for the increased light absorption by PSs, which in turn leads to the increase in singlet oxygen generation.[109]

Geddes and co-workers have done a few studies on MEF-assisted singlet oxygen formation using different PSs. Using Rose Bengal (RB) as PS and green reagent (GR) as singlet oxygen sensor, they studied the extent of singlet oxygen production in close proximity to a Ag film. Upon UV light exposure, the intensity of GR emission on a Ag film was increased by 3.3 times compared with the GR emission on a glass substrate (Figure 11).[109, 119] The distance dependence of MEF was demonstrated by depositing SiO_2 layers of various thicknesses on Ag films. The enhancement of singlet oxygen generation was 1.3 fold for the 5-nm-thick SiO_2 layer, and no enhancement was observed when the thickness of the SiO_2 layer was increased beyond 5 nm. This is due to the electric field enhancement around Ag,

which decreases exponentially away from the surface. The effect of excitation power on the formation of singlet oxygen was studied by exciting RB by 4 mW to 60 mW at 532 nm, and significant enhancement in singlet oxygen production was observed.[120]

Huang *et al.* detected the singlet oxygen formation using Au nanorods (NRs)-conjugated chlorin e6 (Ce6) as PS and 1,3-diphenylisobenzofuran (DPBF) as probe to detect singlet oxygen. The singlet oxygen yield of Au NRs-Ce6 was 1.4 times higher than that of a free Ce6. Here, due to the SPR of Au NRs, they act as nanoantennas to collect more incident photons, and increase the local intensity of excited light, resulting in an enhancement of the fluorescence of the fluorophore and increased singlet oxygen production.[121] Jang *et al.* also utilized Au NRs-PS complex for PDT study. Au NRs were conjugated to mono-methoxy poly(ethylene glycol) and short peptide RRLAC first, followed by introduction of negatively charged PS. *In Vivo* therapeutic study revealed that tumor growth was reduced by 79 % in Au NR-PS treated cells than in free PS treated cells. They argued that when PS are located near the Au NR surface, in addition to enhanced singlet oxygen generation, the energy can be transferred from PS to NR and the PS may become non-fluorescent. So the Au NR-PS becomes non-fluorescent while in the circulatory system PSs are released from Au NR and become fluorescent. The tumor can be detected by fluorescence imaging and selectively destroyed.[110] Using Au NPs, Oo *et al.* demonstrated the formation of reactive oxygen species (ROS). Au NPs were mixed with protoporphyrin IX PS, and dihydrorhodamine-123 (DHR 123) was used as ROS tracking agent. Upon reaction with ROS, non-fluorescent DHR123 can be converted to fluorescent Rhodamine 123 (R123). The enhancement of generation of ROS was maximal for Au NPs having size 106 nm (Figure 12), where the conversion of R123 from DHR123 was proportional to ROS concentration. Clearly, the fluorescent intensity was strongly correlated to the size of Au NPs. This is due to the localized plasmonic field intensity around Au NPs. The intensity of NFE is stronger when the metal NPs are

larger in size.[122]

6.2 SPR-enhanced display devices

Efficient light emission from emitting materials mainly depends on the quantum efficiency, radiative efficiency and current injection efficiency. Increasing the radiative recombination by coupling QDs/dyes to surface plasmons is rather a new approach to improve the performance of display devices. The resonant excitation of SPs by incident light leads to enhancement in light scattering, absorption and local electromagnetic field around the metal NPs.[123] Although coupling of SPs in the metal/dielectric interface is considered as a requirement to match the momentum of incident light to that of SP generated by light, it is not always necessary if the QD/dye is close to the metal. This is because excitation of SPs enhances the density of local fields by concentrating the light, which enhances the emission of fluorophores.[42]

6.2.1 SPR-mediated emission in LEDs

SP-enhanced light emission in LEDs using Ag NPs was studied by Park and co-workers.[63, 124-128] Figure 13 shows the SP-enhanced LEDs with Ag nanoparticles embedded in p-GaN.[125] Enhancement of luminescence in InGaN/GaN quantum well (QW)-LED through QD-SP coupling effect was studied by inserting Ag NPs between n-GaN layer and the InGaN/GaN multiple quantum well (MQW) layer. At an input current of 100 mA, the optical output from this LED was increased by 32.2 % in the presence of a Ag NP layer (Figure 14). The life time of LEDs with Ag NP layer was 80 ps at 330K, while it was 140 ps without Ag NP layer. The decrease in the life time in the presence of Ag is due to the coupling of QW with SPs of Ag NPs. When the exciton energy of QW is close to the SPR energy of metal NPs, the exciton energy can be transferred to the SPs, which leads to the faster PL decay.[63] Coupling of near-ultraviolet (NUV) emission of NUV-LEDs and SPs of metal NPs was demonstrated by growing InGaN/GaN NUV-MQW on substrate first, followed by deposition of 20-nm-thick

p-GaN layer as spacer. A layer of Ag was deposited on the *p*-GaN spacer layer. The optical output was increased by 20.1% with Ag NP layer at an injection current of 20 mA.[124] 38 % increase in the output power was obtained when Ag NPs were deposited on *p*-GaN.[125] A 92 times faster spontaneous emission was observed in InGaN/GaN QW with Ag layer. The resonant enhancement was prominent when Ag-QW separation was 4 nm, which indicates that the coupling between dipole emitters and SP field increases as the distance between QW and Ag decreases.[126] Yeh *et al.* studied the effect of the Ag film thickness on the enhancement of emission of LED. They prepared InGaN/GaN QW LED having different thickness of Ag layers. A sample with 12-nm-thick Ag layer showed maximum PL intensity (Figure 15) and the output efficiency at 20 mA, compared to one with 8 nm- and 10-nm-thick Ag layers.[129] The SP coupled enhancement of emission of LED with Au layers, instead of Ag layers, was studied by Sung *et al*. A Au layer of 2 nm thickness was deposited on InGaN/GaN LED. An enhancement of 180% in electroluminescence intensity was observed for LED sample with a Au layer. In this case SP excitation wavelength of Au does not overlap with the emission wavelength of LED. They concluded that better enhancement in emission can be obtained if the SP excitation wavelength of Au is closer to the emission wavelength of LED, since this can lead to effective SP-QD coupling. It can be assumed that in all the above-mentioned works, the enhancement in optical output of LEDs is due to the resonance coupling between the emission of MQWs and SPs of Ag NPs.[130]

6.2.2 SPR-mediated emission in OLEDs

The important factors that decide the efficiency of OLEDs are the efficiency of the formation of excitons and the efficiency of emission due to the decay of the excitons. Most of the light produced by the decay of excitons are trapped in the devise as waveguide form, and lost into absorption.[105] This poor light extraction efficiency of OLEDs limits the external quantum efficiency. Recently, excitation of SPs as a tool to improve the extraction of light was

explored by a few groups.[61, 131-136] The near field enhancement by plasmonic metals improves the absorbance and emission of dyes in OLEDs, which thus improves the energy transfer in the light emitting device. Yang *et al.* demonstrated the SP induced enhanced energy transfer in a Alq3:DCM-based fluorescent OLED. In order to enhance the Föster process in the donor-acceptor system of OLEDs, Ag NPs were chosen since the SP wavelength of Ag is overlapped with the absorption range of the acceptor and the emission of the donor. An enhancement of 3.5 fold was obtained for the sample with Ag cluster, compared to the sample without Ag clusters. The donor decay rate increases as the SP excitation wavelength moves closer to the donor emission wavelength, and the donor-acceptor interaction is enhanced when the SP energy becomes closer to the absorption energy of the acceptor. These two processes attributed to the improved energy transfer between the donor and the acceptor, which in turn enhances the optical output of the OLED.[61] In another work they deposited Ag NPs of various size and density on the cathode having LiF spacer to study exciton emission/SP coupling effects for a donor-only system (Figure 16),[61] and obtained 1.75 fold increased emission, compared to the structure without Ag clusters. Since LSPR depends on the cluster size and spacing between the clusters, sample 3, which has high density of Ag clusters compared to that of sample 1 and 2, showed better output emission owing to larger particle size and narrower spacing between neighboring clusters (Figure 17).[132] Feng *et al*. obtained 10 times enhancement of emission intensity when a dye-doped dielectric acceptor layer was deposited onto the surface of the Ag cathode, and the acceptor was deposited on the other side of the metallic film. 10 times enhancement of emission was obtained when the donor and the acceptor were separated by the Ag cathode. This result was ascribed to the coupled SPs on the opposite interface of the Ag cathode, which act as efficient channel for the transfer of energy from the donor to the acceptor.[133]

7. Conclusions and outlook

We tried to comprehensively overview the possibilities to influence the luminescence of emitters in the presence of plasmonic metals in this review. The metal-emitter architectures may offer enhanced synergistic optical performance such as increased quantum yield, increased rates of excitation and reduced lifetime, provided that the spatial distribution of the metal and the emitter are properly engineered. Quenching of emission is observed when the emitter is located very close to the metal due to the transfer of emission energy from the dyes/QDs to the metal, which was further explained by NSET mechanism. The enhancement of emission was explained via the two most plausible mechanisms, *i.e.*, RET and NFE. Coupling between SPs and molecular dipoles leads to RET, whereas dyes/QDs experience enhanced excitation when they are in the enhanced electromagnetic field around the plasmonic nanostructures. The influence of NFE can improve FRET efficiency also by changing the excitation and decay rate of the donor and the acceptor. Quenching of FRET driven by the presence of plasmonic metals is mainly due to NSET. In the last section we discussed a few SPR-based theranosis and display applications. The diverse hybrid structures that have been reported here include mainly Au and Ag as plasmonic nanostructures since they allow feasible overlapping of SP excitation wavelength with the absorption or emission of the donor or acceptor. Recent works of various groups that showed SPR-induced enhanced performance for viable applications were discussed in each section.

In spite of partial success in SPR-induced improved performance of luminescence toward analytical tools and display devises, many issues regarding the architectural control over the metal-emitter still remain as practical challenges. To exploit the full potential of MEF, identifying suitable preparation parameters and optimizing the size, shape and distance between the various components of the fluorophore ensemble are the key subjects to be resolved. Considering all the wide possibilities and applications of SPR-induced enhancement of the luminescence of dyes/QDs, we strongly believe that a careful designing

and coupling of SP-QD/dye will open widespread real-life applications in the near future.

ACKNOWLEDGMENTS

This work was supported by the National Research Foundation of Korea Grant funded by the Korean government (2011-0029409).

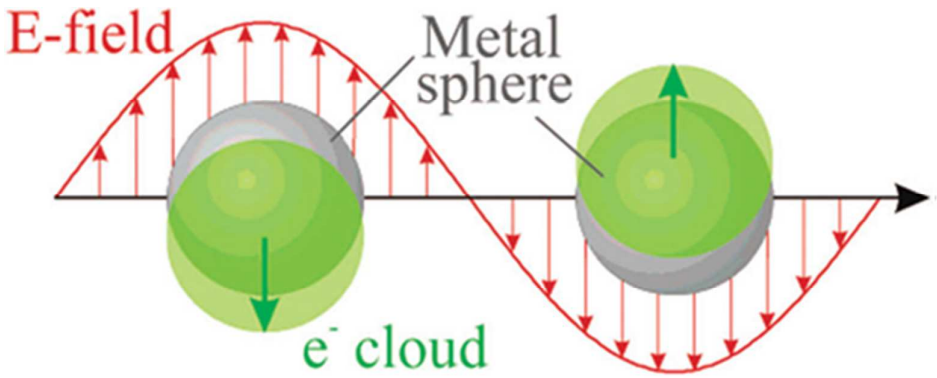

Scheme 1: Schematic of plasmon oscillation for a sphere, showing the displacement of the conduction electron charge cloud relative to the nuclei. Reprinted with permission from ref. [24]. Copyright 2003, American Chemical Society.

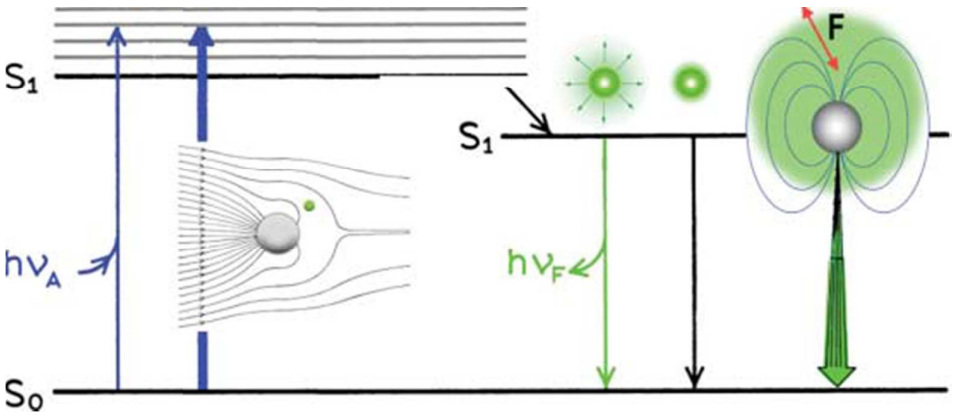

Scheme 2: Modified Jablonski diagram which includes metal−fluorophore interactions. The thicker arrows represent increased rates of excitation and emission. Reprinted with permission from ref.[33]. Copyright 2009, WILEY-VCH Verlag GmbH & Co. KGaA, Weinheim.

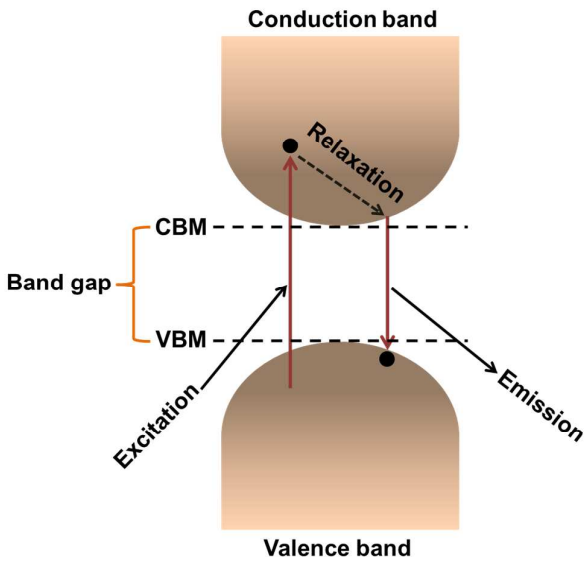

Scheme 3: Schematic representation of photoluminescence process in semiconductors. CBM and VBM represent conduction band minimum and valence band maximum, respectively. The distance between VBM and CBM is called as band gap.

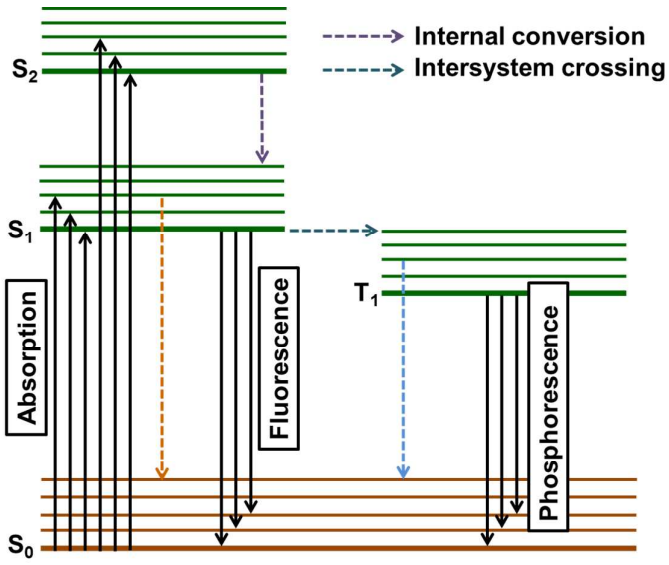

Scheme 4: Jablonski diagram showing the various steps involved in fluorescence and phosphorescence. S_0 denotes singlet ground state, S_1 and S_2 are the excited singlet states. T represents triplet states. Internal conversion and intersystem crossing are non-radiative processes. Intersystem crossings are accompanied by a forbidden change in the spin state, which later leads to phosphorescence.

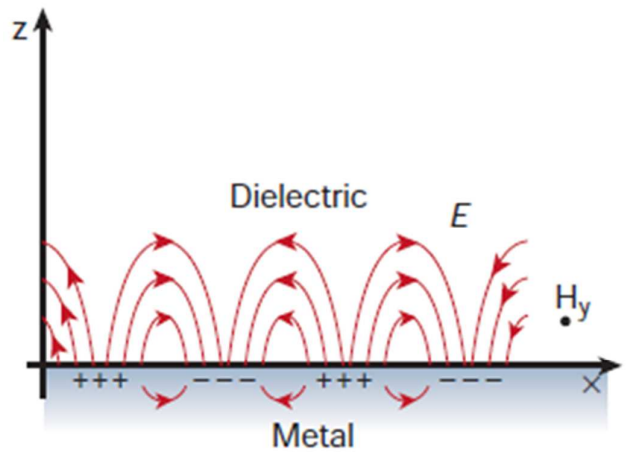

Scheme 5: SPP as a collective excitation at a metal−dielectric interface. The electromagnetic field (electric field, E, plotted in the z−x plane; magnetic field, H_y, sketched in the y direction) is drastically enhanced. SPs at the interface between a metal and a dielectric material have a combined character of electromagnetic wave and surface charge. Reprinted with permission from ref.[26]. Copyright 2003, Nature Publishing Group.

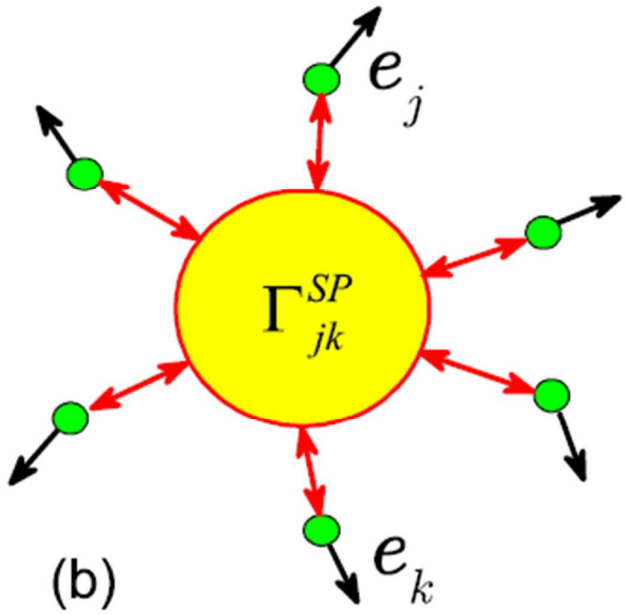

Scheme 6: Schematic representation of the plasmonic coupling of emitters near a metal NP. Reprinted with permission from ref.[30]. Copyright 2010, American Physical Society.

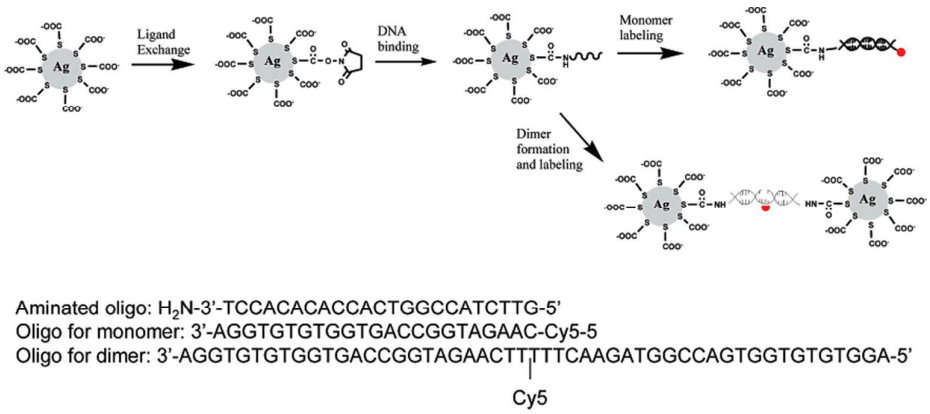

Aminated oligo: H_2N-3'-TCCACACACCACTGGCCATCTTG-5'
Oligo for monomer: 3'-AGGTGTGTGGTGACCGGTAGAAC-Cy5-5
Oligo for dimer: 3'-AGGTGTGTGGTGACCGGTAGAACTTTTTCAAGATGGCCAGTGGTGTGTGGA-5'
Cy5

Scheme 7: The tiopronin-coated silver particle was succinimidylated via ligand exchange, covalently bound with aminated single-stranded oligonucleotide by condensation, and fluorescently labeled by complementary single-stranded cy5-labeled oligonucleotide to generate the labeled metal monomer. Reprinted with permission from ref .[23]. Copyright 2007, American Chemical Society.

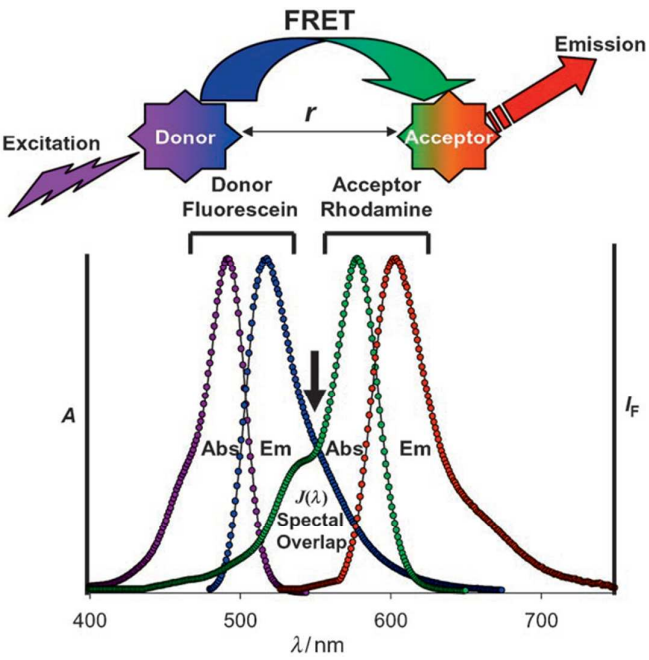

Scheme 8: Schematic of the FRET process: Upon excitation, the excited state donor molecule transfers energy non-radiatively to a proximal acceptor molecule located at distance r from the donor. The acceptor releases the energy either through fluorescence or non-radiative channels. The spectra show the absorption (Abs) and emission (Em) profiles of one of the most commonly used FRET pairs: fluorescein as donor and rhodamine as acceptor. Reprinted with permission from ref.[137]. Copyright 2006, WILEY-VCH Verlag GmbH & Co. KGaA, Weinheim.

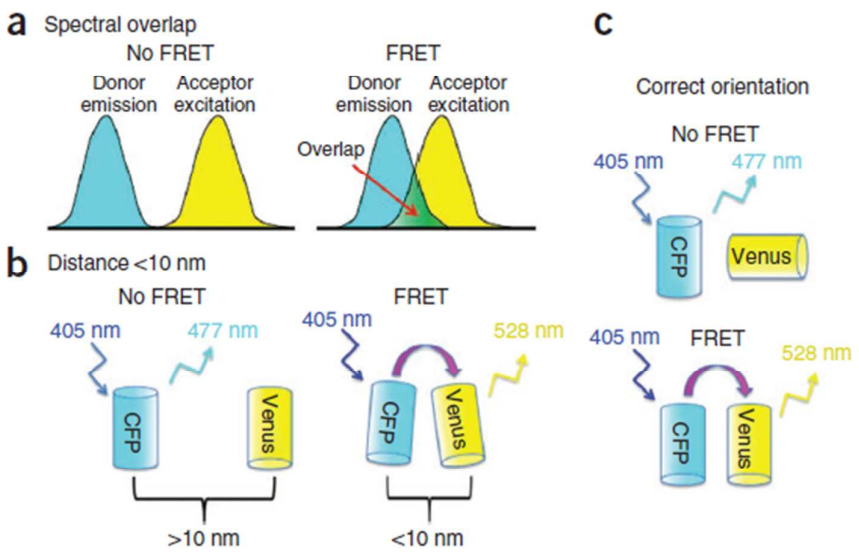

Scheme 9: Schematic diagrams depicting the three conditions that should be required for efficient FRET. (a) The emission spectrum from the donor fluorophore must overlap with the excitation spectrum of the acceptor fluorophore. (b) If the donor and acceptor are within ~10 nm of one another, then energy transfer can occur from the donor (CFP) to the acceptor (Venus). (c) If the donor and acceptor fluorophore dipoles are parallel to each other, FRET is occurred. Reprinted with permission from ref.[85]. Copyright 2013, Nature Publishing Group.

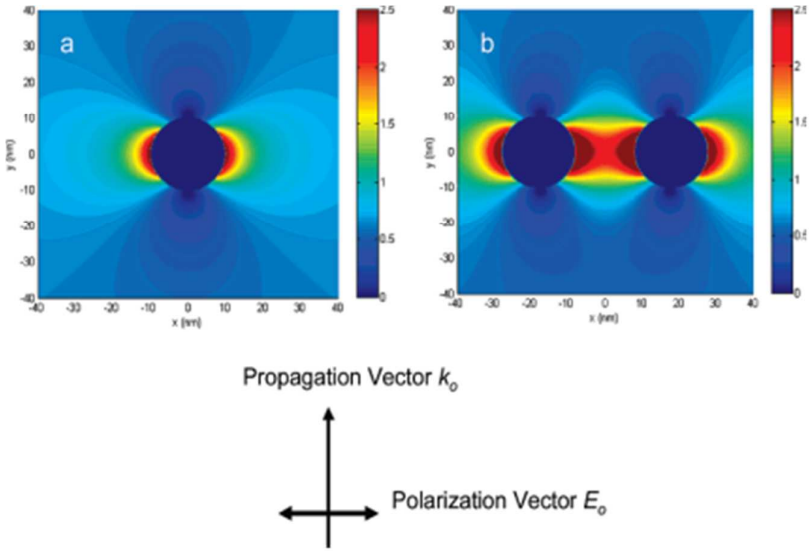

Figure 1: Electric fields near silver (a) monomer and (b) dimer were calculated by FDTD model under an incident light of 635 nm. Reprinted with permission from ref.[23]. Copyright 2007, American Chemical Society.

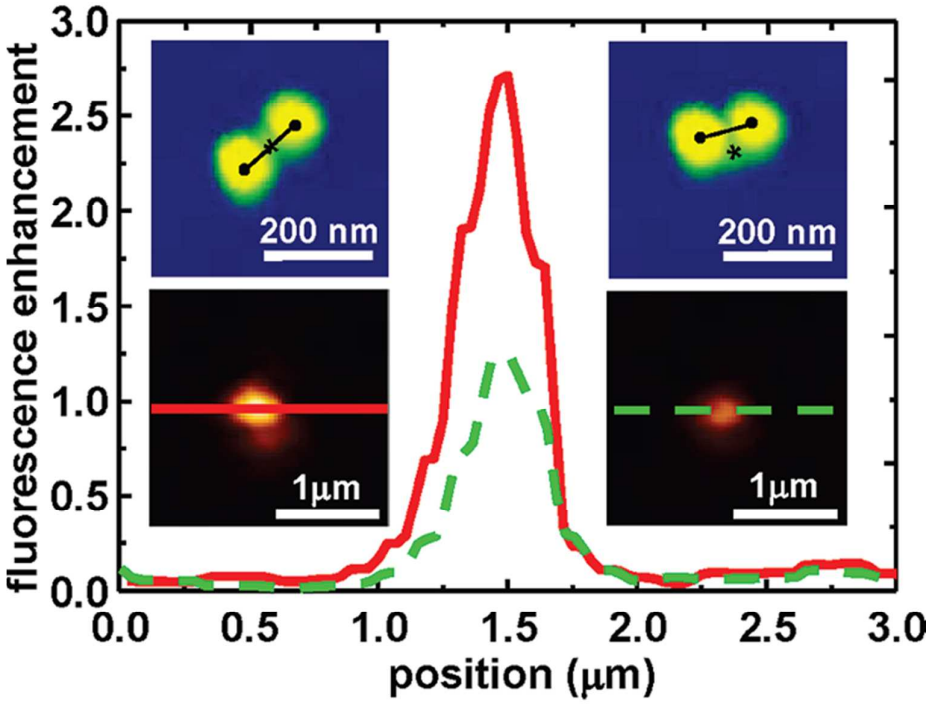

Figure 2. (a) The fluorescence enhancement is very sensitive to the exact placement of the FS between the Au NPs. The graph shows fluorescence intensities obtained with two different FS positions. The AFM height images are shown in the upper two insets, and the corresponding fluorescence images are shown in the lower two insets. The exact positions of the AuNPs and the FS are indicated by solid black dots and asterisks, respectively. The axis connecting the two Au NP centers is also indicated. In the left column, the FS is sandwiched in the hot spot right between the two Au NPs, which leads to a strong fluorescence enhancement (solid red line). In the right column, the FS is not in the hot spot, and consequently, the fluorescence enhancement is less pronounced (dashed green line). Reprinted with permission from ref.[75]. Copyright 2008, American Chemical Society.

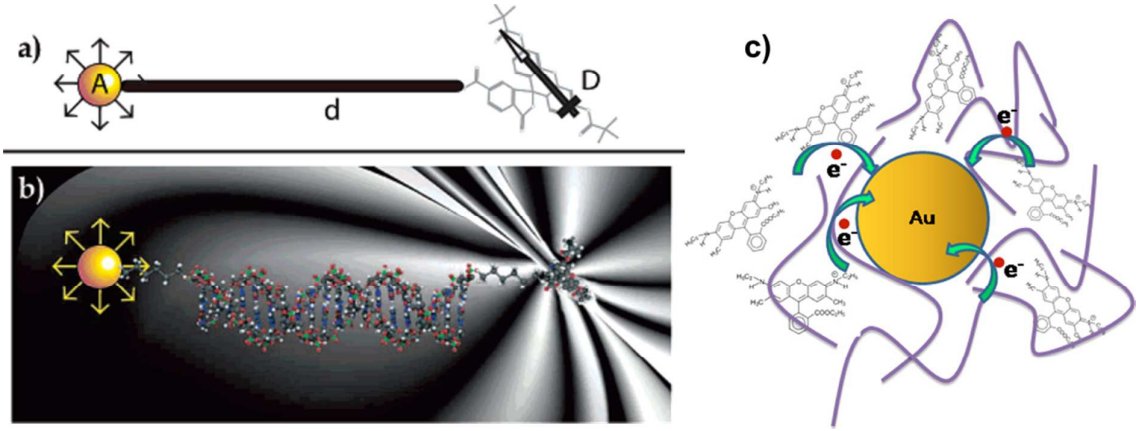

Figure 3. (a) Graphic representation of a donor dye-nanometal acceptor pair separated by dsDNA approximated as a rigid rod of length, *d*. The donor is treated as a localized dipole, and the acceptor is assumed to have overlap at all stearadians. (b) Pictorial representation of a gold NP in an idealized electric field of a nearby molecular dipole. All surface dipole scattering events associated with the free electrons of the gold are shown perpendicular to the surface, which are predicted to be the dominant contributors to the NSET process. Reprinted with permission from ref.[45]. Copyright 2006, American Chemical Society. (c) Schematic diagram of the electron transfer in rhodamine 6G doped Au nanocomposite polymers. Reprinted with permission from ref.[83]. Copyright 2010, AIP publishing.

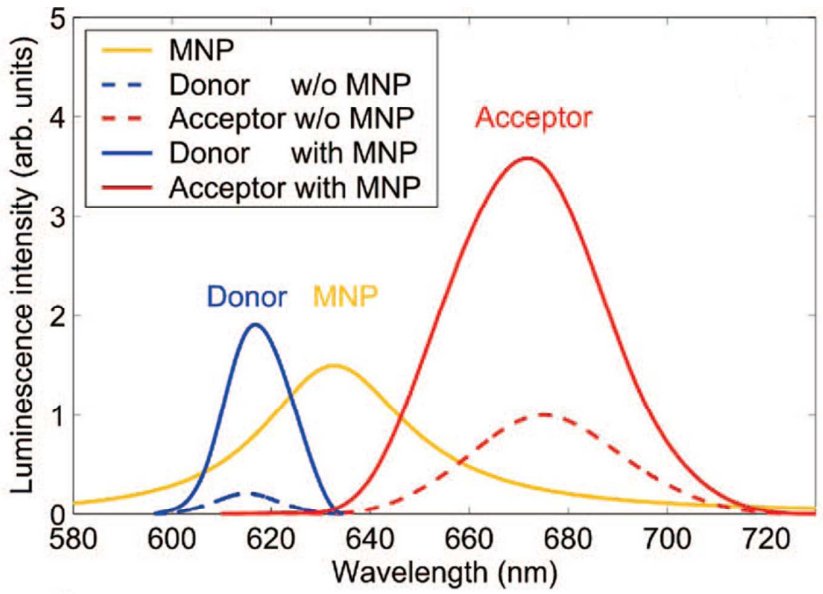

Figure 4. Fluorescence spectra with (solid lines) and without (dashed lines) the metallic nanoparticle. The bright, orange line indicates the scattered intensity of the metallic nanoparticle in absence of donor and acceptor molecules. Reprinted with permission from ref.[32]. Copyright 2008, American Chemical Society.

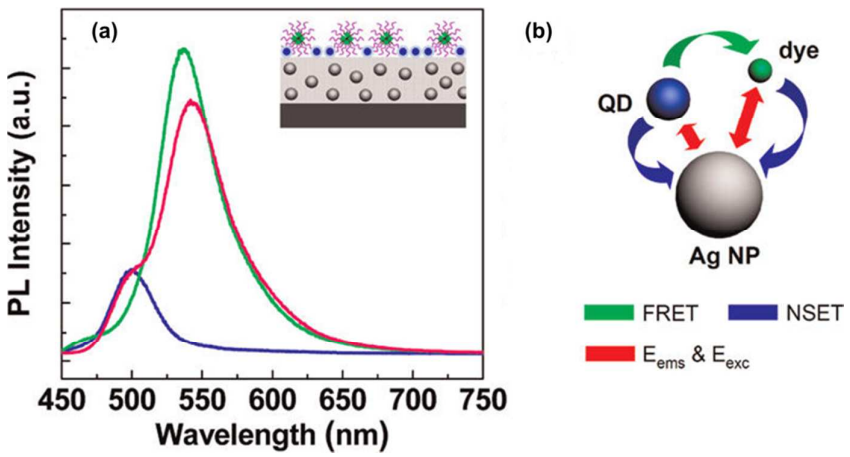

Figure 5: (a) Steady-state fluorescence spectra from a single-layered film of micelles on a NP film with only QDs (blue), with only dyes (green), and with QDs and dyes (pink). (b) Schematics of near-field interactions among QDs, dyes, and Ag NPs in the micellar hybrid. Green, blue, and red arrows were used for presenting FRET, NSET, and excitation/emission enhancement factors, respectively. Reprinted with permission from ref.[103]. Copyright 2012, American Chemical Society.

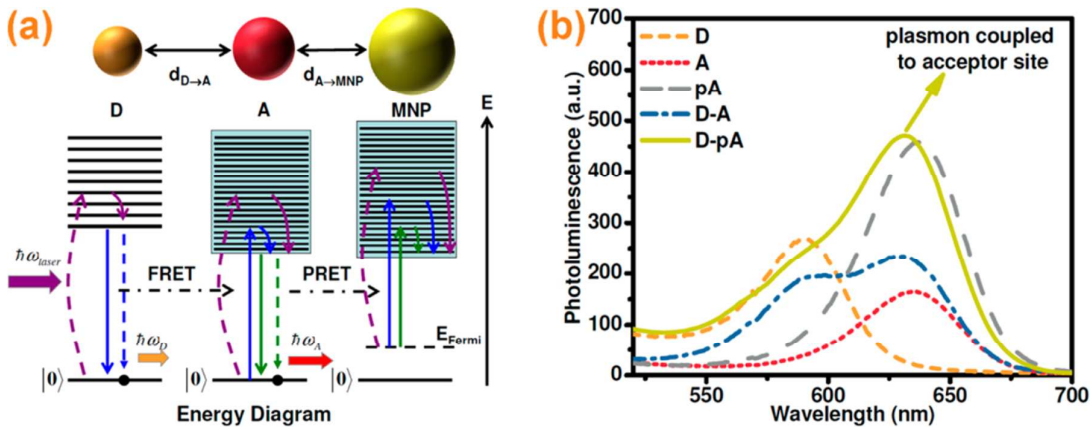

Figure 6. (a) Schematic representation of a donor−acceptor (D−A) energy transfer pair in the case of plasmon coupling to only acceptor QD along with an energy band diagram with the absorption process of the MNP/donor QD/acceptor QD, fast relaxation process, light emission process, energy transfer from the donor to the acceptor and the Coulomb interaction between the donor and acceptor pairs are shown. In the energy diagram, the discrete energy levels for the QDs are depicted, as well as the energy level for the localized plasmons within the continuous energy band of the MNP. (b) Photoluminescence (PL) spectra of the D (dotted orange), A (dotted red), D−A QD pair (dashed blue) under Fo□rster-type energy transfer, plasmon-coupled A (dashed gray), and FRET for the D−A QD pair when only the acceptor QD is coupled to MNP (solid yellow). Reprinted with permission from ref.[95]. Copyright 2013, American Chemical Society.

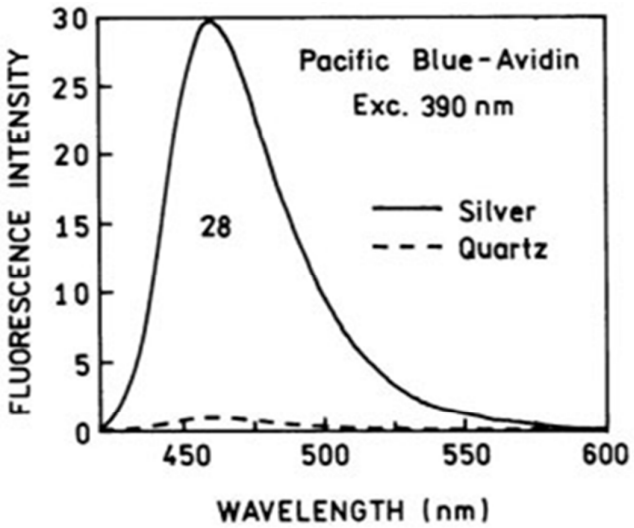

Figure 7. Emission spectra of labeled avidin molecules bound to BSA-coated silver island films. Reprinted with permission from ref.[114]. Copyright 2003, WILEY-VCH Verlag GmbH & Co. KGaA, Weinheim.

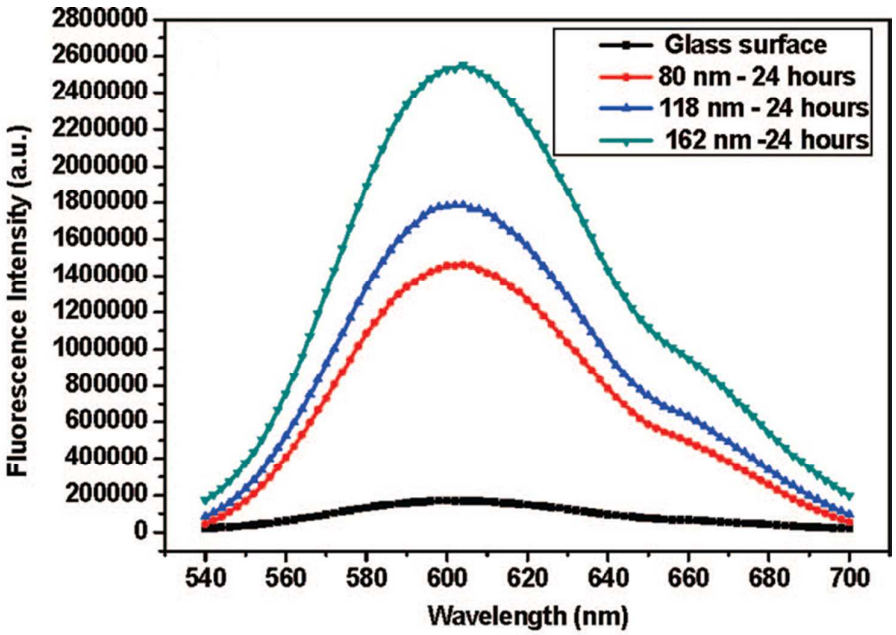

Figure 8. Fluorescence emission intensity of DP-BSA monolayer coating on 162, 118, and 80 nm Au colloid with 24 h incubation time. Reprinted with permission from ref.[116]. Copyright 2008, American Chemical Society.

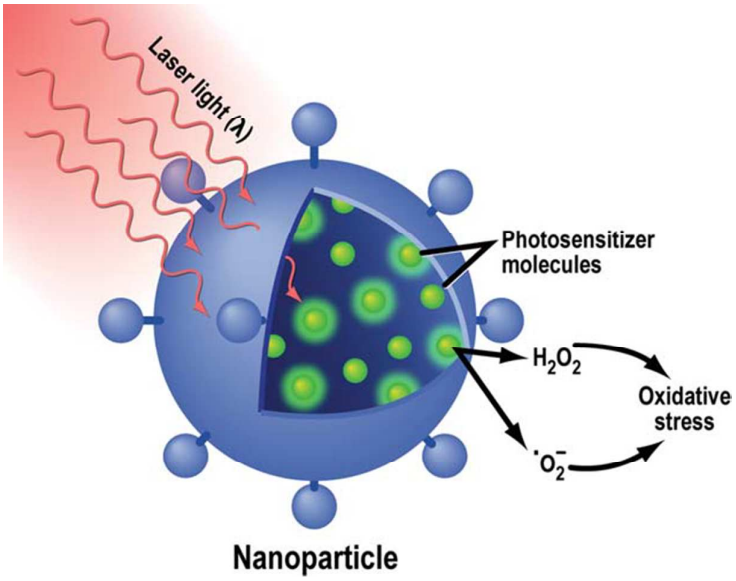

Figure 9. Metal NPs in photodynamic therapy. NPs can deliver light-activatable chemicals, known as photosensitizer molecules, to tumor cells for use in photodynamic therapy. After the absorption of light, photosensitizer molecules can generate cytotoxic oxygen-based reactive species, which can subsequently cause cellular damage and cell death via oxidative stress. Reprinted with permission from ref.[108]. Copyright 2013, American Cancer Society.

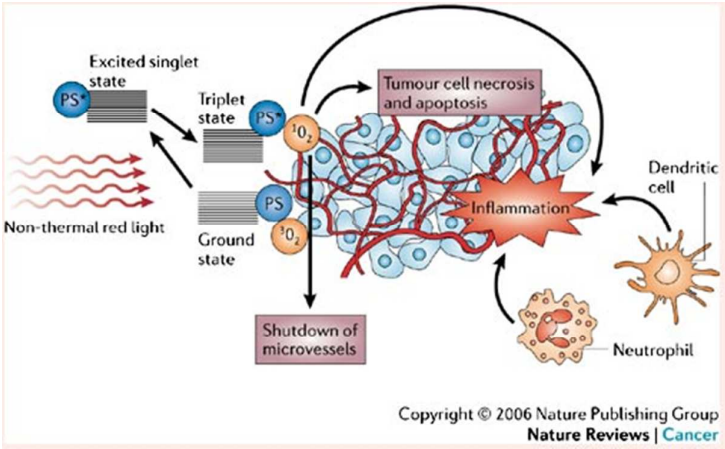

Figure 10. The photosensitizer (PS) absorbs light and an electron moves to the first short-lived excited singlet state. This is followed by intersystem crossing, in which the excited electron changes its spin and produces a longer-lived triplet state. The PS triplet transfers energy to the ground-state triplet oxygen, which produces reactive singlet oxygen ($^1O_2$). $^1O_2$ can directly kill tumour cells by the induction of necrosis and/or apoptosis, can cause destruction of tumour vasculature and produces an acute inflammatory response that attracts leukocytes such as dendritic cells and neutrophils. Reprinted with permission from ref.[118]. Copyright 2006, Nature Publishing Group.

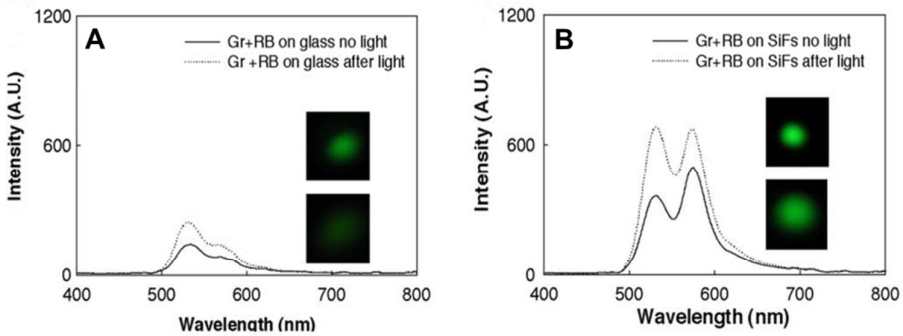

Figure 11. Fluorescence emission spectra of mixture of green sensor (Gr) and RB, both on glass (A), silver film (B). Reprinted with permission from ref.[109]. Copyright 2008, National Academy of Science, U. S. A..

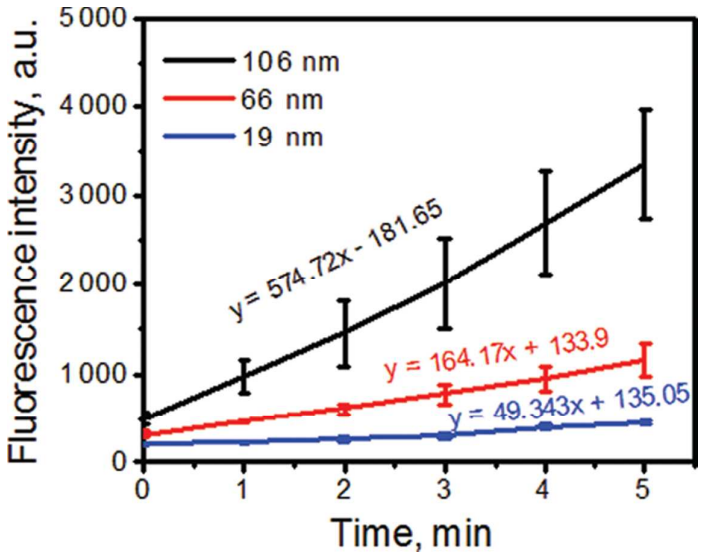

Figure 12. Change in the fluorescent intensity due to the formation of conversion of DHR 123 to R-123 upon reaction with ROS. Reprinted with permission from ref.[122]. Copyright 2012, American Chemical Society.

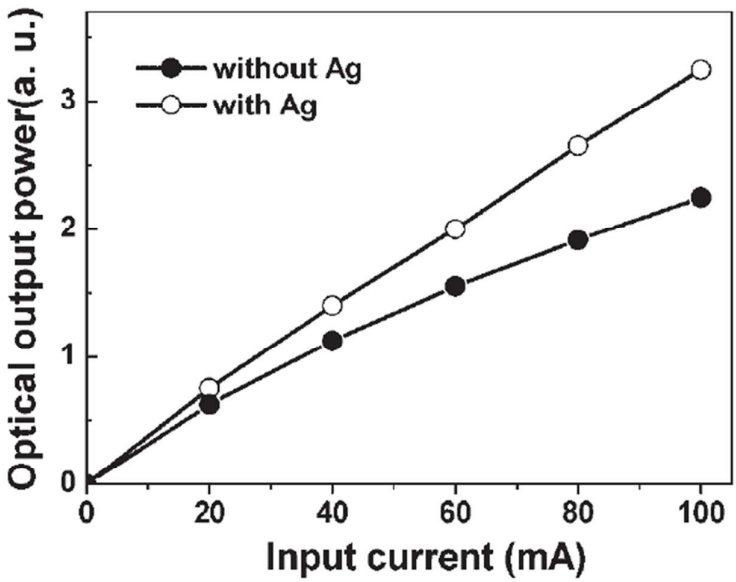

Figure 13. Output power characteristics of InGaN/GaN MQW LEDs with Ag nanoparticles (white-dotted line) and without Ag nanoparticles (black dotted line). Reprinted with permission from ref.[63]. Copyright 2008, WILEY-VCH Verlag GmbH & Co. KGaA, Weinheim.

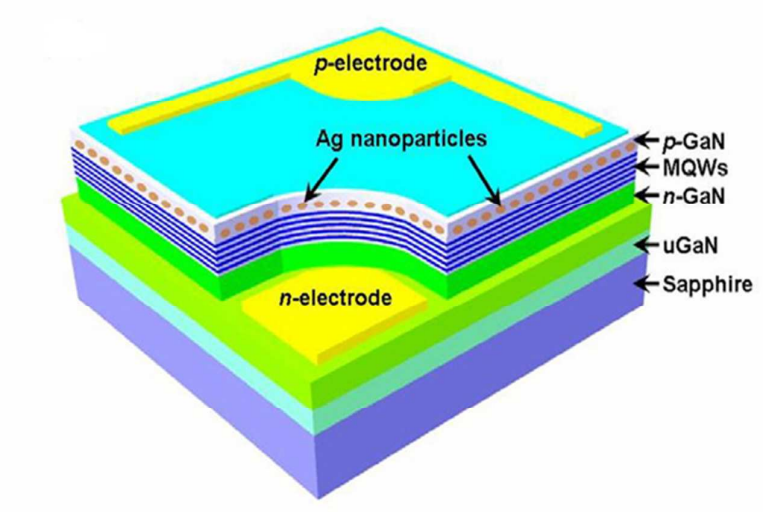

Figure 14. Schematic illustration of SP-enhanced LEDs with Ag nanoparticles embedded in p-GaN. Reprinted with permission from ref.[125]. Copyright 2010, IOP Publishing.

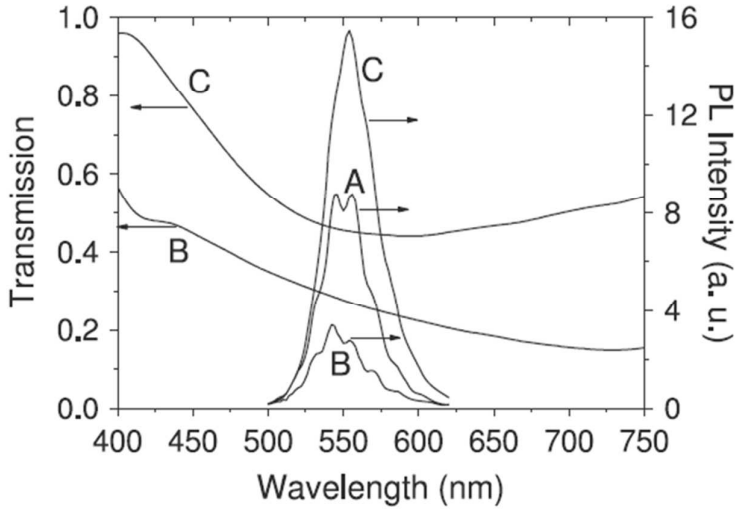

Figure 15. Room temperature PL spectra (right ordinate) of the three LED samples showing their relative intensities. The transmission spectra (left ordinate) of LED samples B and C. Reprinted with permission from ref.[129]. Copyright 2008, IOP Publishing.

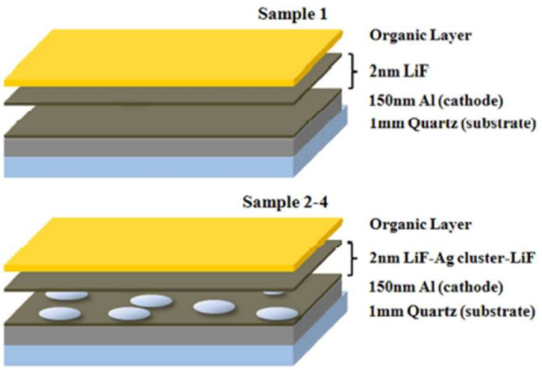

Figure 16. Schematics of samples with different Ag deposition conditions in OLED structures. Reprinted with permission from ref.[61]. Copyright 2009, OSA Publishing.

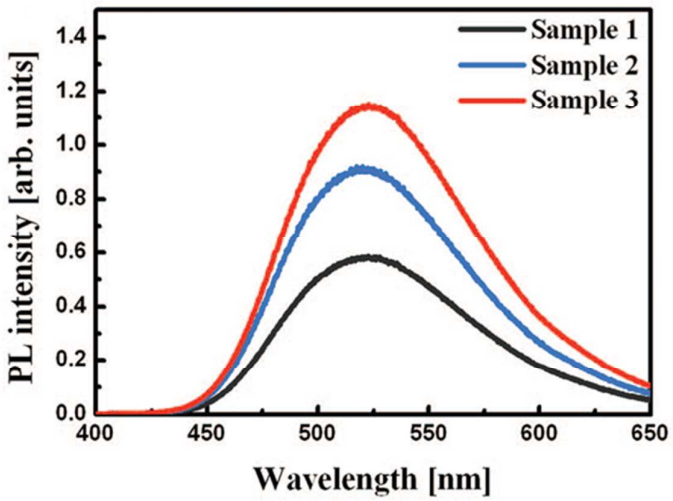

Figure 17. Room temperature PL spectra of samples 1–3 of different resonance wavelengths. Excitation wavelength was 266 nm. Reprinted with permission from ref.[132]. Copyright 2009, AIP Publishing.

8. References

1. S. Dhoble, H. Swart and K. Park, *Phosphate Phosphors for Solid-state Lighting*, Springer, 2012.
2. R. C. Ropp, *Luminescence and the solid state*, Elsevier Amsterdam, 1991.
3. J. Heine and K. Müller-Buschbaum, *Chem. Soc. Rev.*, 2013, **42**, 9232.
4. J. R. Lakowicz, *Principles of fluorescence spectroscopy*, Springer, 2009.
5. B. Valeur, *Molecular fluorescence: principles and applications*, John Wiley & Sons, 2013.
6. D. Darvill, A. Centeno and F. Xie, *Phys. Chem. Chem. Phys.*, 2013, **15**, 15709.
7. Y. Li, A. Rizzo, R. Cingolani and G. Gigli, *Microchimica Acta*, 2007, **159**, 207.
8. N. Tokmoldin, N. Griffiths, D. D. Bradley and S. A. Haque, *Adv. Mater.*, 2009, **21**, 3475.
9. J. Caruge, J. Halpert, V. B. V Wood, cacute and M. Bawendi, *Nat. Photonics*, 2008, **2**, 247.
10. Q. Sun, Y. A. Wang, L. S. Li, D. Wang, T. Zhu, J. Xu, C. Yang and Y. Li, *Nat. Photonics*, 2007, **1**, 717.
11. L. Qian, Y. Zheng, J. Xue and P. H. Holloway, *Nat. Photonics*, 2011, **5**, 543.
12. X. Ji, J. Zheng, J. Xu, V. K. Rastogi, T.-C. Cheng, J. J. DeFrank and R. M. Leblanc, *J. Phys. Chem. B*, 2005, **109**, 3793.
13. R. Freeman, R. Gill, I. Shweky, M. Kotler, U. Banin and I. Willner, *Angew. Chem.*, 2009, **121**, 315.
14. W. R. Algar, A. J. Tavares and U. J. Krull, *Anal. Chim. Acta*, 2010, **673**, 1.
15. A. C. Samia, X. Chen and C. Burda, *J. Am. Chem. Soc.*, 2003, **125**, 15736.
16. H.-C. Huang, S. Barua, G. Sharma, S. K. Dey and K. Rege, *J. Controlled Release*, 2011, **155**, 344.

17. R. Bardhan, N. K. Grady, J. R. Cole, A. Joshi and N. J. Halas, *ACS Nano*, 2009, **3**, 744.
18. F. Tam, G. P. Goodrich, B. R. Johnson and N. J. Halas, *Nano Lett.*, 2007, **7**, 496.
19. W. Deng, F. Xie, H. T. Baltar and E. M. Goldys, *Phys. Chem. Chem. Phys.*, 2013, **15**, 15695.
20. Y. Chen, K. Munechika and D. S. Ginger, *Nano Lett.*, 2007, **7**, 690.
21. P. Reineck, D. Gómez, S. H. Ng, M. Karg, T. Bell, P. Mulvaney and U. Bach, *ACS Nano*, 2013, **7**, 6636.
22. E. Dulkeith, M. Ringler, T. Klar, J. Feldmann, A. Munoz Javier and W. Parak, *Nano Lett.*, 2005, **5**, 585.
23. J. Zhang, Y. Fu, M. H. Chowdhury and J. R. Lakowicz, *Nano Lett.*, 2007, **7**, 2101.
24. K. L. Kelly, E. Coronado, L. L. Zhao and G. C. Schatz, *J. Phys. Chem. B*, 2003, **107**, 668.
25. M. E. Stewart, C. R. Anderton, L. B. Thompson, J. Maria, S. K. Gray, J. A. Rogers and R. G. Nuzzo, *Chem. Rev.*, 2008, **108**, 494.
26. W. L. Barnes, A. Dereux and T. W. Ebbesen, *Nature*, 2003, **424**, 824.
27. S. Eustis and M. A. El-Sayed, *Chem. Soc. Rev.*, 2006, **35**, 209.
28. E. Hutter and J. H. Fendler, *Adv. Mater.*, 2004, **16**, 1685.
29. V. N. Pustovit and T. V. Shahbazyan, *Phys. Rev. B*, 2011, **83**, 085427.
30. V. N. Pustovit and T. V. Shahbazyan, *Phys. Rev. B*, 2010, **82**, 075429.
31. T. Ming, L. Zhao, Z. Yang, H. Chen, L. Sun, J. Wang and C. Yan, *Nano Lett.*, 2009, **9**, 3896.
32. F. Reil, U. Hohenester, J. R. Krenn and A. Leitner, *Nano Lett.*, 2008, **8**, 4128.
33. J. Lakowicz and Y. Fu, *Laser Photonics Rev.*, 2009, **3**, 221.
34. M. Lessard-Viger, M. Rioux, L. Rainville and D. Boudreau, *Nano Lett.*, 2009, **9**, 3066.

35. M. L. Viger, D. Brouard and D. Boudreau, *J. Phys. Chem. C*, 2011, **115**, 2974.

36. B. Meer, G. Coker and S.-Y. S. Chen, *Cambridge: VCH*, 1994.

37. J. R. Lakowicz, K. Ray, M. Chowdhury, H. Szmacinski, Y. Fu, J. Zhang and K. Nowaczyk, *Analyst*, 2008, **133**, 1308.

38. L. Bergman and J. L. McHale, *Handbook of luminescent semiconductor materials*, CRC Press, 2012.

39. K. K. Smith, *Thin Solid Films*, 1981, **84**, 171.

40. J. R. Lakowicz, Y. Shen, S. D'Auria, J. Malicka, J. Fang, Z. Gryczynski and I. Gryczynski, *Anal. Biochem.*, 2002, **301**, 261.

41. X. Hua, J. Gersten and A. Nitzan, *J. Chem. Phys.*, 1985, **83**, 3650.

42. W. Barnes, *J. Mod. Opt.*, 1998, **45**, 661.

43. O. Benson, *Nature*, 2011, **480**, 193.

44. J. R. Lakowicz, *Anal. Biochem.*, 2005, **337**, 171.

45. T. Jennings, M. Singh and G. Strouse, *J. Am. Chem. Soc.*, 2006, **128**, 5462.

46. C. Yun, A. Javier, T. Jennings, M. Fisher, S. Hira, S. Peterson, B. Hopkins, N. Reich and G. Strouse, *J. Am. Chem. Soc.*, 2005, **127**, 3115.

47. I. Pockrand, A. Brillante and D. Möbius, *Chem. Phys. Lett.*, 1980, **69**, 499.

48. Y. Jin and X. Gao, *Nat. Nanotechnol.*, 2009, **4**, 571.

49. Y. D. Han, J. W. Lee, D. H. Park, S. H. Yang, B. K. Kim, J. Kim and J. Joo, *Synth. Met.*, 2011, **161**, 2103.

50. M. Kondon, J. Kim, N. Udawatte and D. Lee, *J. Phys. Chem. C*, 2008, **112**, 6695.

51. P. Pompa, L. Martiradonna, A. Della Torre, F. Della Sala, L. Manna, M. De Vittorio, F. Calabi, R. Cingolani and R. Rinaldi, *Nat. Nanotechnol.*, 2006, **1**, 126.

52. O. Muskens, V. Giannini, J. Sanchez-Gil and J. Gomez Rivas, *Nano Lett.*, 2007, **7**, 2871.

53. N. T. Fofang, T.-H. Park, O. Neumann, N. A. Mirin, P. Nordlander and N. J. Halas, *Nano Lett.*, 2008, **8**, 3481.

54. N. J. Halas, S. Lal, W.-S. Chang, S. Link and P. Nordlander, *Chem. Rev.*, 2011, **111**, 3913.

55. V. N. Pustovit and T. V. Shahbazyan, *Phys. Rev. Lett.*, 2009, **102**, 077401.

56. J. Zhang, Y. Fu, M. H. Chowdhury and J. R. Lakowicz, *J. Phys. Chem. C*, 2007, **111**, 11784.

57. K. H. An, M. Shtein and K. P. Pipe, *Opt. Express18*, 2010, **4041**.

58. K. K. Haldar, T. Sen and A. Patra, *J. Phys. Chem. C*, 2010, **114**, 4869.

59. O. Kulakovich, N. Strekal, A. Yaroshevich, S. Maskevich, S. Gaponenko, I. Nabiev, U. Woggon and M. Artemyev, *Nano Lett.*, 2002, **2**, 1449.

60. I. Gryczynski, J. Malicka, Y. Shen, Z. Gryczynski and J. R. Lakowicz, *J. Phys. Chem. B*, 2002, **106**, 2191.

61. K. Y. Yang, K. C. Choi and C. W. Ahn, *Opt. Express*, 2009, **17**, 11495.

62. J. R. Lakowicz, J. Kuśba, Y. Shen, J. Malicka, S. D'Auria, Z. Gryczynski and I. Gryczynski, *J. Fluoresc*, 2003, **13**, 69.

63. M. K. Kwon, J. Y. Kim, B. H. Kim, I. K. Park, C. Y. Cho, C. C. Byeon and S. J. Park, *Adv. Mater.*, 2008, **20**, 1253.

64. R. Swathi and K. Sebastian, *J. Chem. Phys.*, 2007, **126**, 234701.

65. S. Bhowmick, S. Saini, V. B. Shenoy and B. Bagchi, *J. Chem. Phys.*, 2006, **125**, 181102_1.

66. A. P. Demchenko, *Methods Appl. Fluoresc*, 2013, **1**, 022001.

67. P. Bharadwaj and L. Novotny, *Opt. Express*, 2007, **15**, 14266.

68. Y. Shen, J. Swiatkiewicz, T.-C. Lin, P. Markowicz and P. N. Prasad, *J. Phys. Chem. B*, 2002, **106**, 4040.

69. H. Raether, *Surface plasmons on smooth surfaces*, Springer, 1988.

70. H. Ditlbacher, N. Felidj, J. Krenn, B. Lamprecht, A. Leitner and F. Aussenegg, *Appl. Phys. B*, 2001, **73**, 373.

71. Y.-P. Hsieh, C.-T. Liang, Y.-F. Chen, C.-W. Lai and P.-T. Chou, *Nanotechnology*, 2007, **18**, 415707.

72. S. El-Bashir, F. Barakat and M. AlSalhi, *J. Lumin.*, 2013, **143**, 43.

73. J.-H. Song, T. Atay, S. Shi, H. Urabe and A. V. Nurmikko, *Nano Lett.*, 2005, **5**, 1557.

74. V. Giannini, A. Berrier, S. A. Maier, J. A. Sánchez-Gil and J. G. Rivas, *Opt. Express*, 2010, **18**, 2797.

75. A. Bek, R. Jansen, M. Ringler, S. Mayilo, T. A. Klar and J. Feldmann, *Nano Lett.*, 2008, **8**, 485.

76. S. Gresillon, L. Aigouy, A. Boccara, J. Rivoal, X. Quelin, C. Desmarest, P. Gadenne, V. Shubin, A. Sarychev and V. M. Shalaev, *Phys. Rev. Lett.*, 1999, **82**, 4520.

77. K. Sokolov, G. Chumanov and T. M. Cotton, *Anal. Chem.*, 1998, **70**, 3898.

78. D. P. Fromm, A. Sundaramurthy, P. J. Schuck, G. Kino and W. Moerner, *Nano Lett.*, 2004, **4**, 957.

79. A. Kinkhabwala, Z. Yu, S. Fan, Y. Avlasevich, K. Müllen and W. Moerner, *Nat. Photonics*, 2009, **3**, 654.

80. P. Anger, P. Bharadwaj and L. Novotny, *Phys. Rev. Lett.*, 2006, **96**, 113002.

81. S. Chowdhury, Z. Wu, A. Jaquins-Gerstl, S. Liu, A. Dembska, B. A. Armitage, R. Jin and L. A. Peteanu, *J. Phys. Chem. C*, 2011, **115**, 20105.

82. E. Dulkeith, A. Morteani, T. Niedereichholz, T. Klar, J. Feldmann, S. Levi, F. Van Veggel, D. Reinhoudt, M. Möller and D. Gittins, *Phys. Rev. Lett.*, 2002, **89**, 203002.

83. B. Karthikeyan, *J. Appl. Phys.*, 2010, **108**, 084311.

84. D. J. Maxwell, J. R. Taylor and S. Nie, *J. Am. Chem. Soc.*, 2002, **124**, 9606.

85. J. A. Broussard, B. Rappaz, D. J. Webb and C. M. Brown, *Nat. Protocols*, 2013, **8**, 265.

86. S. M. Müller, H. Galliardt, J. Schneider, B. G. Barisas and T. Seidel, *Front. Plant Sci.*, 2013, **4**.

87. K. Truong and M. Ikura, *Curr. Opin. Struct. Biol.*, 2001, **11**, 573.

88. R. N. Day, A. Periasamy and F. Schaufele, *Methods*, 2001, **25**, 4.

89. A. Giannetti, L. Citti, C. Domenici, L. Tedeschi, F. Baldini, M. B. Wabuyele and T. Vo-Dinh, *Sens. Actuators. B*, 2006, **113**, 649.

90. D. Kajihara, R. Abe, I. Iijima, C. Komiyama, M. Sisido and T. Hohsaka, *Nat. Methods*, 2006, **3**, 923.

91. J. R. Lakowicz, J. Malicka, S. D'Auria and I. Gryczynski, *Anal. Biochem.*, 2003, **320**, 13.

92. S. Chatterjee, J. B. Lee, N. V. Valappil, D. Luo and V. M. Menon, *Biomed. Opt. Express*, 2011, **2**, 1727.

93. A. Wokaun, H. P. Lutz, A. King, U. Wild and R. Ernst, *J. Chem. Phys.*, 1983, **79**, 509.

94. M. Lunz, X. Zhang, V. A. Gerard, Y. K. Gun'ko, V. Lesnyak, N. Gaponik, A. S. Susha, A. L. Rogach and A. L. Bradley, *J. Phys. Chem. C*, 2012, **116**, 26529.

95. T. Ozel, P. L. Hernandez Martinez, E. Mutlugun, O. Akin, S. Nizamoglu, I. O. Ozel, Q. Zhang, Q. Xiong and H. V. Demir, *Nano Lett.*, 2013.

96. A. O. Govorov, J. Lee and N. A. Kotov, *Phys. Rev. B*, 2007, **76**, 125308.

97. L. Zhao, T. Ming, L. Shao, H. Chen and J. Wang, *J. Phys. Chem. C*, 2012, **116**, 8287.

98. J. I. Gersten and A. Nitzan, *Chem. Phys. Lett.*, 1984, **104**, 31.

99. M. Lunz, V. A. Gerard, Y. K. Gun'ko, V. Lesnyak, N. Gaponik, A. S. Susha, A. L. Rogach and A. L. Bradley, *Nano Lett.*, 2011, **11**, 3341.

100. V. Faessler, C. Hrelescu, A. Lutich, L. Osinkina, S. Mayilo, F. Jäckel and J. Feldmann,

Chem. Phys. Lett., 2011, **508**, 67.

101. X.-R. Su, W. Zhang, L. Zhou, X.-N. Peng and Q.-Q. Wang, *Opt. Express*, 2010, **18**, 6516.

102. X.-R. Su, W. Zhang, L. Zhou, X.-N. Peng, D.-W. Pang, S.-D. Liu, Z.-K. Zhou and Q.-Q. Wang, *Appl. Phys. Lett.*, 2010, **96**, 043106.

103. K.-S. Kim, J.-H. Kim, H. Kim, F. d. r. Laquai, E. Arifin, J.-K. Lee, S. I. Yoo and B.-H. Sohn, *ACS Nano*, 2012, **6**, 5051.

104. X. Zhang, C. A. Marocico, M. Lunz, V. A. Gerard, Y. K. Gun'ko, V. Lesnyak, N. Gaponik, A. S. Susha, A. L. Rogach and A. L. Bradley, *ACS Nano*, 2012, **6**, 9283.

105. P. A. Hobson, S. Wedge, J. A. Wasey, I. Sage and W. L. Barnes, *Adv. Mater.*, 2002, **14**, 1393.

106. M. Ganguly, C. Mondal, J. Chowdhury, J. Pal, A. Pal and T. Pal, *Dalton Trans.*, 2014, **43**, 1032.

107. E. M. Goldys, K. Drozdowicz-Tomsia, F. Xie, T. Shtoyko, E. Matveeva, I. Gryczynski and Z. Gryczynski, *J. Am. Chem. Soc.*, 2007, **129**, 12117.

108. A. S. Thakor and S. S. Gambhir, *CA-Cancer J. Clin.*, 2013, **63**, 395.

109. Y. Zhang, K. Aslan, M. J. Previte and C. D. Geddes, *PNAS*, 2008, **105**, 1798.

110. B. Jang, J.-Y. Park, C.-H. Tung, I.-H. Kim and Y. Choi, *ACS Nano*, 2011, **5**, 1086.

111. K. Aslan, I. Gryczynski, J. Malicka, E. Matveeva, J. R. Lakowicz and C. D. Geddes, *Curr. Opin. Biotechnol.*, 2005, **16**, 55.

112. J. Malicka, I. Gryczynski, C. D. Geddes and J. R. Lakowicz, *J. Biomed. Opt.*, 2003, **8**, 472.

113. J. Malicka, I. Gryczynski and J. R. Lakowicz, *Biochem. Biophys. Res. Commun.*, 2003, **306**, 213.

114. B. P. Maliwal, J. Malicka, I. Gryczynski, Z. Gryczynski and J. R. Lakowicz,

Biopolymers, 2003, **70**, 585.

115. F. Xie, M. S. Baker and E. M. Goldys, *J. Phys. Chem. B*, 2006, **110**, 23085.

116. F. Xie, M. S. Baker and E. M. Goldys, *Chem. Mater.*, 2008, **20**, 1788.

117. Y. Zhang, K. Aslan, M. J. Previte, S. N. Malyn and C. D. Geddes, *J. Phys. Chem. B*, 2006, **110**, 25108.

118. A. P. Castano, P. Mroz and M. R. Hamblin, *Nat. Rev. Cancer*, 2006, **6**, 535.

119. Y. Zhang, K. Aslan, M. J. Previte and C. D. Geddes, *J. Fluoresc*, 2007, **17**, 345.

120. J. Karolin and C. D. Geddes, *Phys. Chem. Chem. Phys.*, 2013, **15**, 15740.

121. X. Huang, X.-J. Tian, W.-l. Yang, B. Ehrenberg and J.-Y. Chen, *Phys. Chem. Chem. Phys.*, 2013.

122. M. K. Khaing Oo, Y. Yang, Y. Hu, M. Gomez, H. Du and H. Wang, *ACS Nano*, 2012, **6**, 1939.

123. B. H. Kim, C. H. Cho, J. S. Mun, M. K. Kwon, T. Y. Park, J. S. Kim, C. C. Byeon, J. Lee and S. J. Park, *Adv. Mater.*, 2008, **20**, 3100.

124. S. Nakamura, T. Mukai and M. Senoh, *Appl. Phys. Lett.*, 1994, **64**, 1687.

125. C.-Y. Cho, M.-K. Kwon, S.-J. Lee, S.-H. Han, J.-W. Kang, S.-E. Kang, D.-Y. Lee and S.-J. Park, *Nanotechnology*, 2010, **21**, 205201.

126. A. Neogi, C.-W. Lee, H. O. Everitt, T. Kuroda, A. Tackeuchi and E. Yablonovitch, *Phys. Rev. B*, 2002, **66**, 153305.

127. C. H. Lu, C. C. Lan, Y. L. Lai, Y. L. Li and C. P. Liu, *Adv. Funct. Mater.*, 2011, **21**, 4719.

128. C.-Y. Cho, S.-J. Lee, J.-H. Song, S.-H. Hong, S.-M. Lee, Y.-H. Cho and S.-J. Park, *Appl. Phys. Lett.*, 2011, **98**, 051106.

129. D.-M. Yeh, C.-F. Huang, C.-Y. Chen, Y.-C. Lu and C. Yang, *Nanotechnology*, 2008, **19**, 345201.

130. J.-H. Sung, B.-S. Kim, C.-H. Choi, M.-W. Lee, S.-G. Lee, S.-G. Park, E.-H. Lee and O. Beom-Hoan, *Microelectron. Eng.*, 2009, **86**, 1120.

131. D. Zhang, Y. Li and J. Tang, *J. Mater. Chem. C*, 2013.

132. K. Y. Yang, K. C. Choi and C. W. Ahn, *Appl. Phys. Lett.*, 2009, **94**, 173301.

133. J. Feng, T. Okamoto, R. Naraoka and S. Kawata, *Appl. Phys. Lett.*, 2008, **93**, 051106.

134. J. Feng, T. Okamoto and S. Kawata, *Appl. Phys. Lett.*, 2005, **87**, 241109.

135. Y. Xiao, J. Yang, P. Cheng, J. Zhu, Z. Xu, Y. Deng, S. Lee, Y. Li and J. Tang, *Appl. Phys. Lett.*, 2012, **100**, 013308.

136. D. K. Gifford and D. G. Hall, *Appl. Phys. Lett.*, 2002, **81**, 4315.

137. K. E. Sapsford, L. Berti and I. L. Medintz, *Angew. Chem. Int. Ed*, 2006, **45**, 4562.